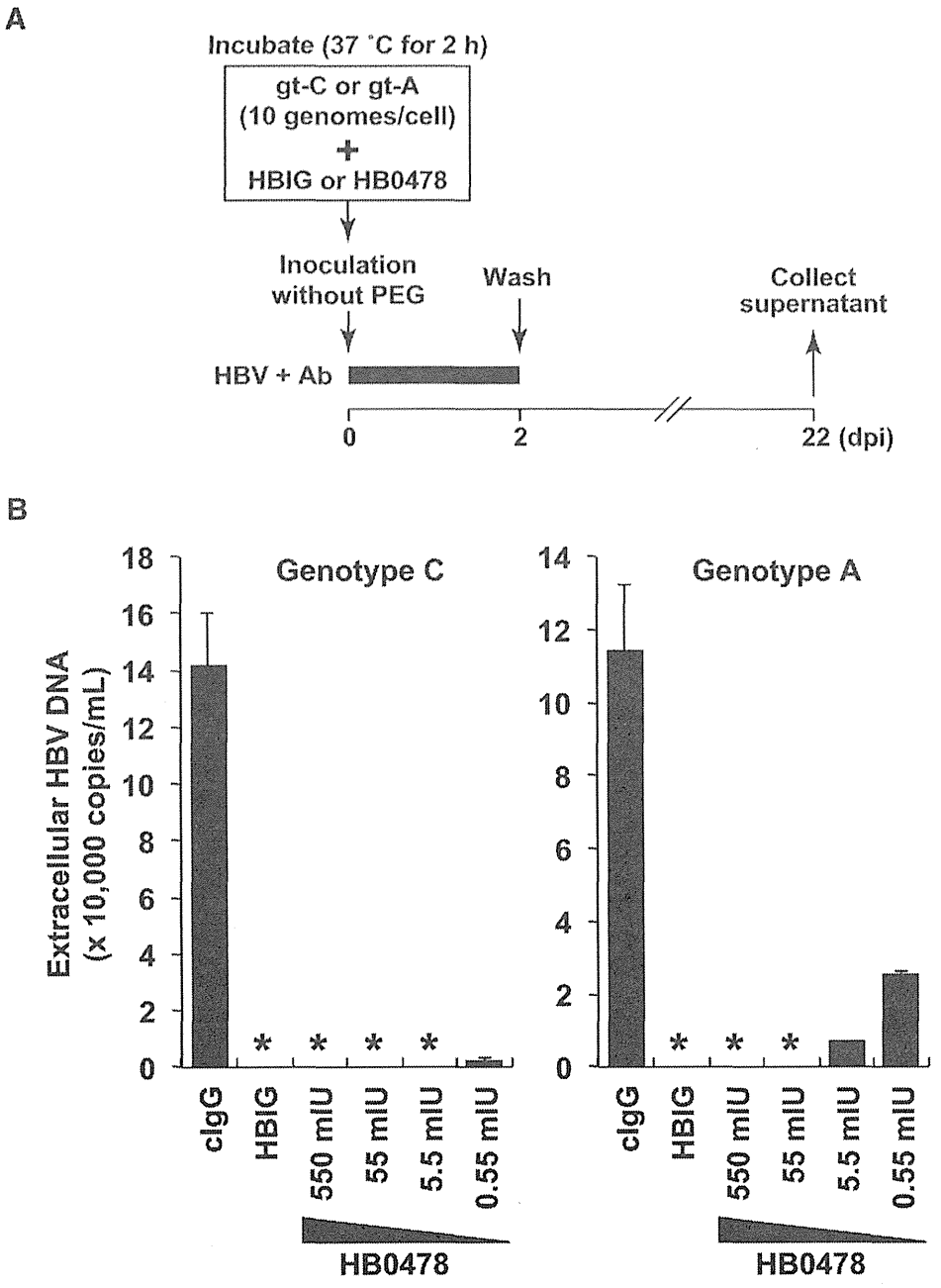

Fig 4. Titration of neutralization of gt-C and gt-A infection by mAb HB0478. HBV gt-C and gt-A were preincubated for 2 hours with 670 ng of control human IgG (cIgG), 100 mIU of HBIG, or 670, 67, 6.7 or 0.67 ng HB0478 (corresponding to 550, 55, 5.5, and 0.55 mIU) and PHHs were inoculated with the products at 10 genomes per cell. The Y-axis depicts the levels of extracellular HBV DNA in the supernatant harvested on 12 days post infection. Asterisks indicate values under the detection limit.

doi:10.1371/journal.pone.0118062.g004

Meanwhile, virus strains with amino acid substitutions in HBsAg often escape from HB vaccine-induced antibody and HBIG treatment during vertical transmission of HBV [19,20,29]. The substitution reported most frequently is residue 145, glycine to arginine (G145R), located in the second loop of the "a" determinant of HBsAg. This study demonstrated that HB0478 also recognized HBsAg with the G145R substitution and protected against G145R infection in vivo, whereas HB0116 did not bind to the G145R substituted protein or neutralize the mutant. Although how G145R in the second loop affects mAb-binding to the first loop is largely unknown, it is possible that the C(K/R)TC-dependent HB0478 epitope might be more distant from the second loop than that of HB0116, suggesting that HB0478 might not be affected by the conformational change of HBsAg induced by substitution of glycine at residue 145. It is noted that epitopes other than "a" determinant such as those within pre-S2 region [30] could also contributed to the neutralization of escape mutants.

In conclusion, this study raises the possibility that active immunization with a gt-C-based vaccine confers prophylaxis against gt-A, which is spreading in Japan, and against escape mutants such as G145R, when the anti-HBs responses are sufficient. Note that PHHs isolated from chimeric mice with human hepatocytes enabled us to investigate precisely the inhibitory effects of the mAbs, or any antiviral compounds, against HBV infection in vitro.

Author Contributions

Conceived and designed the experiments: SHT EI SM KT TJ YT. Performed the experiments: SHT EI TW SM KM KT TO. Analyzed the data: SHT EI TW SM MI SI TI KM. Contributed reagents/materials/analysis tools: HK AM. Wrote the paper: SHT EI TW YT.

References

1. Miyakawa Y, Mizokami M (2003) Classifying hepatitis B virus genotypes. Intervirology 46: 329–338. PMID: 14688448
2. Kim BK, Revill PA, Ahn SH (2011) HBV genotypes: relevance to natural history, pathogenesis and treatment of chronic hepatitis B. Antivir Ther (Lond) 16: 1169–1186. doi: 10.3851/IMP1982 PMID: 22155900
3. Kurbanov F, Tanaka Y, Mizokami M (2010) Geographical and genetic diversity of the human hepatitis B virus. Hepatol Res 40: 14–30. doi: 10.1111/j.1872-034X.2009.00601.x PMID: 20156297
4. Yan H, Zhong G, Xu G, He W, Jing Z, et al. (2012) Sodium taurocholate cotransporting polypeptide is a functional receptor for human hepatitis B and D virus. Elife 1: e00049. doi: 10.7554/eLife.00049 PMID: 23150796
5. Shokrgozar MA, Shokri F (2002) Subtype specificity of anti-HBs antibodies produced by human B-cell lines isolated from normal individuals vaccinated with recombinant hepatitis B vaccine. Vaccine 20: 2215–2220. PMID: 12009275
6. Zanetti AR, Van Damme P, Shouval D (2008) The global impact of vaccination against hepatitis B: a historical overview. Vaccine 26: 6266–6273. doi: 10.1016/j.vaccine.2008.09.056 PMID: 18848855
7. Cassidy A, Mossman S, Olivieri A, De Ridder M, Leroux-Roels G (2011) Hepatitis B vaccine effectiveness in the face of global HBV genotype diversity. Expert Rev Vaccines 10: 1709–1715. doi: 10.1586/erv.11.151 PMID: 22085174
8. Ogata N (2009) [Comparison of antibody responses to hepatitis B surface antigen among four recipient groups of hepatitis B vaccines that have been approved in Japan: evaluation using passive hemagglutination assay and chemiluminescent immunoassay]. Rinsho Byori 57: 954–960. PMID: 19928491
9. Avazova D, Kurbanov F, Tanaka Y, Sugiyama M, Radchenko I, et al. (2008) Hepatitis B virus transmission pattern and vaccination efficiency in Uzbekistan. J Med Virol 80: 217–224. PMID: 18098129
10. Matsuura K, Tanaka Y, Hige S, Yamada G, Murawaki Y, et al. (2009) Distribution of hepatitis B virus genotypes among patients with chronic infection in Japan shifting toward an increase of genotype A. J Clin Microbiol 47: 1476–1483. doi: 10.1128/JCM.02081-08 PMID: 19297602
11. Jin A, Ozawa T, Tajiri K, Obata T, Kondo S, et al. (2009) A rapid and efficient single-cell manipulation method for screening antigen-specific antibody-secreting cells from human peripheral blood. Nat Med 15: 1088–1092. doi: 10.1038/nm.1966 PMID: 19684583

12. Tajiri K, Kishi H, Tokimitsu Y, Kondo S, Ozawa T, et al. (2007) Cell-microarray analysis of antigen-specific B-cells: single cell analysis of antigen receptor expression and specificity. Cytometry A 71: 961–967. PMID: 17910063

13. Tokimitsu Y, Kishi H, Kondo S, Honda R, Tajiri K, et al. (2007) Single lymphocyte analysis with a microwell array chip. Cytometry A 71: 1003–1010. PMID: 17972305

14. Tajiri K, Ozawa T, Jin A, Tokimitsu Y, Minemura M, et al. (2010) Analysis of the epitope and neutralizing capacity of human monoclonal antibodies induced by hepatitis B vaccine. ANTIVIRAL RESEARCH 87: 40–49. doi: 10.1016/j.antiviral.2010.04.006 PMID: 20412816

15. Mercer DF, Schiller DE, Elliott JF, Douglas DN, Hao C, et al. (2001) Hepatitis C virus replication in mice with chimeric human livers. Nat Med 7: 927–933. PMID: 11479625

16. Sugiyama M, Tanaka Y, Kurbanov F, Maruyama I, Shimada T, et al. (2009) Direct cytopathic effects of particular hepatitis B virus genotypes in severe combined immunodeficiency transgenic with urokinase-type plasminogen activator mouse with human hepatocytes. Gastroenterology 136: 652–62.e653. doi: 10.1053/j.gastro.2008.10.048 PMID: 19041311

17. Allweiss L, Volz T, Lutgehetmann M, Giersch K, Bornscheuer T, et al. (2014) Immune cell responses are not required to induce substantial hepatitis B virus antigen decline during pegylated interferon-alpha administration. J Hepatol 60: 500–507. doi: 10.1016/j.jhep.2013.10.021 PMID: 24398036

18. Cooreman MP, Leroux-Roels G, Paulij WP (2001) Vaccine- and hepatitis B immune globulin-induced escape mutations of hepatitis B virus surface antigen. J Biomed Sci 8: 237–247. PMID: 11385295

19. Wu C, Deng W, Deng L, Cao L, Qin B, et al. (2012) Amino acid substitutions at positions 122 and 145 of hepatitis B virus surface antigen (HBsAg) determine the antigenicity and immunogenicity of HBsAg and influence in vivo HBsAg clearance. J Virol 86: 4658–4669. doi: 10.1128/JVI.06353-11 PMID: 22301154

20. Komatsu H, Inui A, Sogo T, Konishi Y, Tateno A, et al. (2012) Hepatitis B surface gene 145 mutant as a minor population in hepatitis B virus carriers. BMC Res Notes 5: 22. doi: 10.1186/1756-0500-5-22 PMID: 22233650

21. Gripon P, Rumin S, Urban S, Le Seyec J, Glaise D, et al. (2002) Infection of a human hepatoma cell line by hepatitis B virus. Proc Natl Acad Sci USA 99: 15655–15660. PMID: 12432097

22. Cerec V, Glaise D, Garnier D, Morosan S, Turlin B, et al. (2007) Transdifferentiation of hepatocyte-like cells from the human hepatoma HepaRG cell line through bipotent progenitor. Hepatology 45: 957–967. PMID: 17393521

23. Abe A, Inoue K, Tanaka T, Kato J, Kajiyama N, et al. (1999) Quantitation of hepatitis B virus genomic DNA by real-time detection PCR. J Clin Microbiol 37: 2899–2903. PMID: 10449472

24. Fujiwara K, Tanaka Y, Paulon E, Orito E, Sugiyama M, et al. (2005) Novel type of hepatitis B virus mutation: replacement mutation involving a hepatocyte nuclear factor 1 binding site tandem repeat in chronic hepatitis B virus genotype E. J Virol 79: 14404–14410. PMID: 16254374

25. Laras A, Koskinas J, Dimou E, Kostamena A, Hadziyannis SJ (2006) Intrahepatic levels and replicative activity of covalently closed circular hepatitis B virus DNA in chronically infected patients. Hepatology 44: 694–702. PMID: 16941694

26. Qiu X, Schroeder P, Bridon D (1996) Identification and characterization of a C(K/R)TC motif as a common epitope present in all subtypes of hepatitis B surface antigen. J Immunol 156: 3350–3356. PMID: 8617960

27. Iwarson S, Tabor E, Thomas HC, Goodall A, Waters J, et al. (1985) Neutralization of hepatitis B virus infectivity by a murine monoclonal antibody: an experimental study in the chimpanzee. J Med Virol 16: 89–96. PMID: 2413167

28. Stramer SL, Wend U, Candotti D, Foster GA, Hollinger FB, et al. (2011) Nucleic acid testing to detect HBV infection in blood donors. N Engl J Med 364: 236–247. doi: 10.1056/NEJMoa1007644 PMID: 21247314

29. Lee PI, Chang LY, Lee CY, Huang LM, Chang MH (1997) Detection of hepatitis B surface gene mutation in carrier children with or without immunoprophylaxis at birth. J Infect Dis 176: 427–430. PMID: 9237708

30. Itoh Y, Takai E, Ohnuma H, Kitajima K, Tsuda F (1986) A synthetic peptide vaccine involving the product of the pre-S(2) region of hepatitis B virus DNA: protective efficacy in chimpanzees. Proc Natl Acad Sci USA 83: 9174–9178. PMID: 3466181

Int J Hematol
DOI 10.1007/s12185-015-1750-z

ORIGINAL ARTICLE

Reactivation of hepatitis B virus (HBV) infection in adult T-cell leukemia–lymphoma patients with resolved HBV infection following systemic chemotherapy

Haruhito Totani · Shigeru Kusumoto · Takashi Ishida · Arisa Masuda · Takashi Yoshida · Asahi Ito · Masaki Ri · Hirokazu Komatsu · Shuko Murakami · Masashi Mizokami · Ryuzo Ueda · Akio Niimi · Hiroshi Inagaki · Yasuhito Tanaka · Shinsuke Iida

Received: 8 November 2014 / Revised: 19 January 2015 / Accepted: 21 January 2015

Abstract Reactivation of hepatitis B virus (HBV) infection may occur in adult T-cell leukemia–lymphoma (ATL) patients with resolved HBV infection who receive monotherapy with the anti-CC chemokine receptor 4 monoclonal antibody, mogamulizumab. However, there is little evidence regarding the incidence and characteristics of HBV reactivation in ATL patients receiving systemic chemotherapy, including the use of this antibody. We conducted a retrospective study for 24 ATL patients with resolved HBV infection underwent regular HBV DNA monitoring to assess HBV reactivation in Nagoya City University Hospital between January 2005 and June 2013. With median HBV DNA follow-up of 238 days (range 57–1420), HBV reactivation (defined as the detection of HBV DNA) was observed in three (12.5 %) of 24 patients with resolved HBV infection. No hepatitis due to HBV reactivation occurred in those patients who were diagnosed with HBV DNA levels below 2.1 log copies/mL and who received antiviral drugs. Mogamulizumab was administered prior to HBV reactivation in two of three HBV-reactivated patients. In the mogamulizumab era, further well-designed prospective studies are warranted to estimate the incidence of HBV reactivation and to establish regular HBV DNA monitoring-guided preemptive antiviral therapy for such patients.

Keywords Reactivation · HBV · CCR4 · Mogamulizumab · ATL

H. Totani · S. Kusumoto (✉) · T. Ishida · A. Masuda · T. Yoshida · A. Ito · M. Ri · H. Komatsu · S. Iida
Department of Hematology and Oncology, Nagoya City University Graduate School of Medical Sciences, 1 Kawasumi, Mizuho-chou, Mizuho-ku, Nagoya, Aichi 467-8601, Japan
e-mail: kusshan@rb3.so-net.ne.jp; skusumot@med.nagoya-cu.ac.jp

S. Murakami · Y. Tanaka
Department of Virology and Liver Unit, Nagoya City University Graduate School of Medical Sciences, Nagoya, Japan

M. Mizokami
The Research Center for Hepatitis and Immunology, National Center for Global Health and Medicine, Ichikawa, Japan

R. Ueda
Department of Tumor Immunology, Aichi Medical University School of Medicine, Aichi, Japan

A. Niimi
Department of Respiratory Medicine, Allergy and Rheumatology, Nagoya City University Graduate School of Medical Sciences, Nagoya, Japan

H. Inagaki
Department of Anatomic Pathology and Molecular Diagnostics, Nagoya City University Graduate School of Medical Sciences, Nagoya, Japan

Abbreviations

HBV	Hepatitis B virus
ATL	Adult T-cell leukemia–lymphoma
HBsAg	Hepatitis B surface antigen
Anti-HBc	Antibodies against hepatitis B core antigen
Anti-HBs	Antibodies against hepatitis B surface antigen
CCR4	CC chemokine receptor 4

Introduction

Reactivation of hepatitis B virus (HBV) infection has been reported as a potentially fatal complication of systemic chemotherapy [1–6]. HBV reactivation may occur not only in hepatitis B surface antigen (HBsAg)-positive patients, but also in patients with resolved HBV infection who are seronegative for HBsAg but seropositive for antibodies

Published online: 30 January 2015

against hepatitis B core antigen (anti-HBc) and/or antibodies against HBsAg (anti-HBs).

Chemotherapy containing the anti-CD20 monoclonal antibody, rituximab plus steroids has been shown to be an important risk factor for HBV reactivation in B-cell lymphoma patients with resolved HBV infection [2, 3]. Recently, the anti-CC chemokine receptor 4 (CCR4) monoclonal antibody, mogamulizumab, was developed and introduced into the management of adult T-cell leukemia–lymphoma (ATL) [7–12]. A dose-finding study showed that mogamulizumab monotherapy could induce HBV reactivation-related hepatitis in an ATL patient with resolved HBV infection [9, 13].

However, there is little evidence regarding the incidence and characteristics of HBV reactivation in ATL patients with resolved HBV infection who were receiving systemic chemotherapy including this antibody. We conducted here a retrospective study in a single institution to evaluate the risk of HBV reactivation in these patients who underwent regular monitoring of HBV DNA levels during and after chemotherapy.

Patients and methods

Between January 2005 and June 2013, 66 patients were diagnosed with ATL in Nagoya City University Hospital. Baseline serological markers for HBsAg, anti-HBc, and anti-HBs were measured to evaluate their viral status before systemic chemotherapy. Antiviral prophylaxis was provided to the HBsAg-positive patients before the initiation of systemic chemotherapy. HBV DNA levels were assessed in HBsAg-negative patients who were seropositive for anti-HBc and/or anti-HBs. Patients seronegative for HBsAg but with detectable of HBV DNA were considered to have occult HBV infection, and antiviral prophylaxis was provided to those patients. HBsAg-negative patients seropositive for anti-HBc and/or anti-HBs but without detectable of HBV DNA were considered to have resolved HBV infection and their HBV DNA levels were monitored regularly (monthly in principle) for HBV DNA levels during chemotherapy and at least 1 year after chemotherapy; HBV reactivation was defined as the detection of HBV DNA. If HBV reactivation was confirmed, antiviral drugs were given immediately (preemptive antiviral therapy).

All baseline serological markers of HBsAg, anti-HBc and anti-HBs were measured by the laboratory in this hospital, using the following methods and cut-off values: CLEIA with cut-off values for HBsAg, anti-HBc and anti-HBs were 1.0 C.O.I, 1.0 INH % and 10.0 mIU/mL, respectively, from January 2005 to December 2010, CLEIA with cut-off values for HBsAg, anti-HBc and ant-HBs were 0.03 mIU/mL, 1.0 C.O.I, and 10.0 mIU/mL, respectively, from January 2011.

HBV DNA levels were measured by an outside laboratory (SRL, Inc.; Tokyo, Japan) or by the laboratory in this hospital, using the following methods and cut-off values: transcription-mediated amplification test with a cut-off value of 3.7 LGE/mL from January 2005 to April 2006, Amplicor HBV monitor test with a cut-off value of 2.6 log copies/mL from April 2006 to May 2008, COBAS AmpliPrep/COBAS TaqMan HBV test (v1.0) with a cut-off value of 1.8 log copies/mL from May 2008 to July 2009, and COBAS AmpliPrep/COBAS TaqMan HBV test (v2.0) with a cut-off value of 2.1 log copies/mL from July 2009.

For the analysis of HBV sequences, nucleic acids were extracted from the preserved serum specimens (200 μL) and subjected to PCR to amplify HBV genomes within the short S region [nucleotides (nt) 427–607] and the basal core promoter (BCP)/precore (PC) regions [nt 1628–2047] followed by direct sequencing using the ABI Prism Big Dye ver. 3.1 kit in an ABI 3100 DNA automated sequencer (Applied Biosystems, Foster City, CA). HBV genotypes were determined by molecular evolutionary analysis [14].

To compare the baseline characteristics and ATL treatment of the patients with and without HBV reactivation, we used the Chi-square test and two-sided Fisher's exact test for categorical data, and the Mann–Whitney U test for continuous variables. A two-tailed p value of less than 0.05 was considered statistically significant. All statistical analyses were performed using SPSS (version 22.0) statistical software for Windows, using data fixed on August 31, 2013. This study was approved by the Institutional Review Board of Nagoya City University. All patients gave written informed consent.

Results

The status of HBV infection at baseline was as follows (Fig. 1): HBsAg-positive (n = 2, 3.0 %), HBsAg-negative (n = 63, 95.5 %), and no serological HBV assessment (n = 1, 1.5 %). Of the 63 HBsAg-negative patients, 31 (49.2 %) were anti-HBc positive and/or anti-HBs positive. Of the remaining 32 patients, 31 were anti-HBc negative and anti-HBs negative, and one had no data for anti-HBc and anti-HBs. Because HBV DNA below 1.8 log copies/mL was detected at baseline in one patient who was anti-HBc positive and anti-HBs positive at baseline (and who was therefore judged to have occult HBV infection), antiviral drugs were administered before initiating systemic chemotherapy. Finally, 24 of 31 patients with resolved HBV infection underwent regular HBV DNA monitoring (Fig. 1). For these 24 ATL patients, initial systemic chemotherapy included the following regimens: CHOP (n = 7, 29.2 %), VCAP-AMP-VECP (n = 13, 54.2 %) and others (n = 4, 16.6 %) (Table 1). Systemic chemotherapy was started in 6

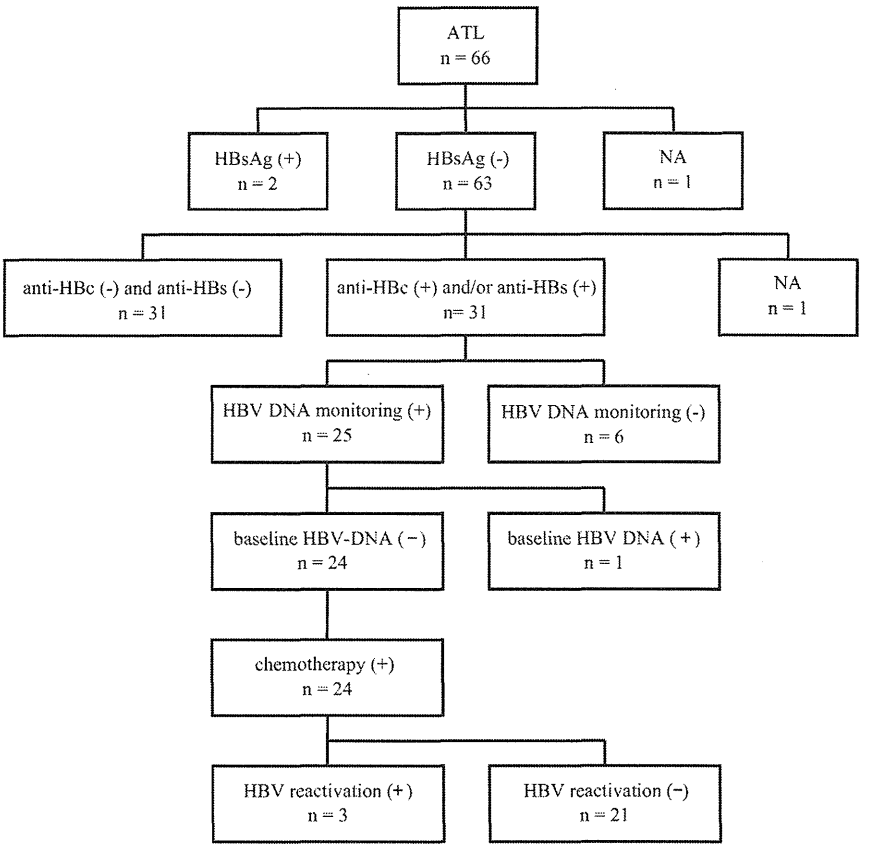

Fig. 1 Baseline serological markers of HBV infection in the 66 ATL patients. Two patients were HBsAg-positive, 63 were HBsAg-negative, the last was not available for serological HBV assessment. Of the 63 HBsAg-negative patients, 31 were anti-HBc-positive and/or anti-HBs-positive. One patient had detectable HBV DNA at baseline, and was judged as having occult HBV infection. Regular HBV DNA monitoring was performed in 24 of 31 patients with resolved HBV infection and 3 patients suffered HBV reactivation. *HBV* hepatitis B virus, *ATL* adult T-cell leukemia–lymphoma, *HBsAg* hepatitis B surface antigen, *anti-HBc* antibodies against hepatitis B core antigen, *anti-HBs* antibodies against hepatitis B surface antigen, *NA* not available

patients before HBV DNA monitoring. For the 24 patients with resolved HBV infection during and after systemic chemotherapy, regular monitoring of HBV DNA was conducted with a median interval of 30 days (range 2–703).

HBV reactivation was observed in 3 (12.5 %) of 24 patients with resolved HBV infection, with a median HBV DNA follow-up of 238 days (range 57–1420). No hepatitis due to HBV reactivation occurred in those patients who were diagnosed with HBV DNA levels below 2.1 log copies/mL and who received antiviral drugs (entecavir, 0.5 mg/day), resulting in no detectable HBV DNA levels during antiviral treatment.

There was no statistically significant difference in baseline characteristics and ATL treatment between patients with and without reactivation in this retrospective analysis (Table 1). The characteristics of 3 patients with HBV reactivation are shown in Table 2; all were male, and seropositive for anti-HBc and anti-HBs at baseline, and received the VCAP-AMP-VECP regimen as initial treatment. Mogamulizumab was administered prior to HBV reactivation in 2 of 3 HBV-reactivated patients. The anti-HBs titers of 3 patients decreased at reactivation compared to baseline titers in 3 patients. Their HBV genotypes were determined as C. HBV mutations were not found in the precore region or basal core promoter. One patient died due to ATL progression.

The clinical course of case 1 is shown in Fig. 2. HBV reactivation was confirmed with HBV DNA levels below 2.1 log copies/mL, 3 months after initiating mogamulizumab-containing chemotherapy as initial treatment for ATL. The patient presented with elevation of transaminase levels after detection of HBV DNA, it considered not viral hepatitis, but drug-induced liver damage because of transient and slight increase of HBV DNA levels. Reemergence of HBV was observed repeatedly after withdrawal of antiviral drugs following the development of drug-induced allergic rash or interstitial pneumonia. The patient maintains complete remission of ATL with undetectable of HBV DNA after withdrawal of antiviral drugs over 3 years after mogamulizumab-containing chemotherapy.

Discussion

This study showed that the incidence of HBV reactivation among ATL patients with resolved HBV infection who received systemic chemotherapy was 12.5 %. Preemptive antiviral therapy, guided by regular HBV DNA monitoring,

Table 1 Baseline characteristics and treatment of 24 ATL patients with resolved HBV infection who underwent HBV DNA monitoring following systemic chemotherapy

	HBV reactivation (+) $n = 3$	HBV reactivation (−) $n = 21$	p value
Median age (range)	59 (58–65)	64 (41–77)	0.822
Sex			0.217
Male	3	9	
Female	0	12	
ATL type of disease			0.090
Acute	1	17	
Lymphoma	2	1	
Chronic	0	2	
Smoldering	0	1	
ECOG performance status			0.530
0 or 1	3	14	
2 or more	0	7	
Baseline HBV status			1.00
Anti-HBc positive and anti-HBs positive	3	18	
Anti-HBc positive and anti-HBs negative	0	3	
Anti-HBc negative and anti-HBs positive	0	0	
Baseline anti-HBs titers (mIU/mL)			0.728
<10	0	3	
≥10, <100	2	8	
≥100	1	10	
Initial chemotherapy regimen[a]			0.396
CHOP	0	7	
VCAP-AMP-VECP	3	10	
Others	0	4	
Mogamulizumab administration[b]			0.576
(+)	2	9	
(−)	1	12	
Allogeneic HSCT[c]			1.00
(+)	1	5	
(−)	2	16	
Year enrolled for HBV DNA monitoring			–
2005–2006	0	0	
2006–2008	0	4	
2008–2009	0	3	
2009–2013	3	14	
Median HBV DNA follow-up time (range)[d]	640 (637–1030)	227 (57–1420)	–

HBV hepatitis B virus, *ATL* adult T-cell leukemia–lymphoma, *ECOG* Eastern Cooperative Oncology Group, *HBsAg* hepatitis B surface antigen, *anti-HBc* antibodies against hepatitis B core antigen, *anti-HBs* antibodies against hepatitis B surface antigen, *CHOP* cyclophosphamide, doxorubicin, vincristine, prednisolone, *VCAP-AMP-VECP* VCAP (vincristine, cyclophosphamide, doxorubicin, prednisolone)-AMP (doxorubicin, ranimustine, prednisolone)-VECP (vindesine, etoposide, carboplatin, prednisolone), *HSCT* hematopoietic stem cell transplantation

[a] Initial chemotherapy regimen for adult T-cell leukemia–lymphoma was given during HBV DNA monitoring

[b] In 2 of 3 HBV-reactivated cases, mogamulizumab was given prior to HBV reactivation

[c] One patient received allogeneic hematopoietic stem transplantation after HBV reactivation

[d] HBV DNA follow-up time indicates the time from the date of baseline HBV DNA measurement until the date of the last HBV DNA measurement

was effective in preventing hepatitis due to HBV reactivation in all three patients. Most of HBV reactivation has been reported to occur in B-cell lymphoma, especially in those who received rituximab-containing chemotherapy [2–4, 6]. This is the first report regarding the risk of HBV reactivation focused on ATL patients with resolved HBV infection, which suggesting that the risk of HBV reactivation in ATL patients may be similar to that in B-cell lymphoma patients [15, 16].

ATL is a mature T-cell lymphoma and human T-cell leukemia virus type-1 plays a role in its pathogenesis. Aggressive ATL has been reported to have a poor prognosis with a median overall survival of approximately 1 year, regardless of intensive chemotherapy [17]. The anti-CCR4 monoclonal antibody, mogamulizumab has been shown recently to be effective and safe for aggressive ATL patients in the setting of monotherapy or combined with conventional chemotherapy [9, 11, 18]. It is expected that mogamulizumab will enable long-term disease control, so more HBV reactivation events may be predicted because CCR4 is a chemokine receptor expressed on T-helper type 2 and regulatory T cells [7, 19], and is thought to have an important

Table 2 Characteristics of 3 patients with HBV reactivation

	Case 1	Case 2	Case 3
Age	65	59	58
Sex	Male	Male	Male
Type of ATL	Lymphoma	Lymphoma	Acute
ECOG performance status	1	1	0
Baseline HBV status			
HBsAg	(−)	(−)	(−)
Anti-HBc titers	98.1 %	3.6 C.O.I	1.5 C.O.I
Anti-HBs titers	20.0 mIU/mL	24.0 mIU/mL	>1000.0 mIU/mL
HBV DNA levels	Not detectable	Not detectable	Not detectable
Chemotherapy regimens before HBV reactivation			
	VCAP-AMP-VECP plus mogamulizumab	VCAP-AMP-VECP	VCAP-AMP-VECP Mogamulizumab CHOP DeVIC etc.
Number of regimens	1	1	7
Allogeneic HSCT[a]	No	Yes	No
After HBV reactivation			
Time to reactivation (day)[b]	90	71	541
HBV DNA levels at reactivation (log copies/mL)	<2.1	<2.1	<2.1
Peak HBV DNA levels (log copies/mL)	2.3	<2.1	<2.1
Anti-HBs titers	17.6 mIU/mL	22.0 mIU/mL	566.5 mIU/mL
HBV genotype	C	C	C
HBV mutation of precore region or basal core promoter	Wild	Wild	NA
Antiviral drugs	Entecavir, lamivudine	Entecavir	Entecavir
Hepatitis due to HBV reactivation	No	No	No
HBV DNA follow-up time (day)[c]	1030	640	637
Outcome	Alive (CR1)	Alive (CR1)	Death due to ATL progression

HBV hepatitis B virus, *ATL* adult T-cell leukemia–lymphoma, *ECOG* Eastern Cooperative Oncology Group, *HBsAg* hepatitis B surface antigen, *anti-HBc* antibodies against hepatitis B core antigen, *anti-HBs* antibodies against hepatitis B surface antigen, *VCAP-AMP-VECP* VCAP (vincristine, cyclophosphamide, doxorubicin, prednisolone)-AMP (doxorubicin, ranimustine, prednisolone)-VECP (vindesine, etoposide, carboplatin, prednisolone), *CHOP* cyclophosphamide, doxorubicin, vincristine, prednisolone, *DeVIC* dexamethasone, etoposide, ifosfamide, carboplatin, *CR1* first complete response

[a] One patient (case 2) received allogeneic hematopoietic stem transplantation after HBV reactivation

[b] Time to reactivation indicates the time from the date of baseline HBV DNA measurement until the date of the confirmation of HBV reactivation

[c] HBV DNA follow-up time indicates the time from the date of baseline HBV DNA measurement until the date of the last HBV DNA measurement

role in maintaining the balance of the human immune system. The mechanism whereby mogamulizumab causes HBV reactivation is not fully understood; a reduction of numbers of CCR4-expressing cells following this antibody treatment might be associated with an imbalance of antiviral immunity, resulting in the development of HBV reactivation [9, 13]. Although HBV reactivation was confirmed in 2 of 11 patients who received mogamulizumab, this study did not prove that HBV reactivation is associated with mogamulizumab therapy, partly because of the small sample size.

This study has the following limitations: a retrospective study in a single institution with a small sample size, and the diagnosis of HBV reactivation at early stage when only when HBV DNA became detectable (below 2.1 log copies/mL) by PCR. Because antiviral treatments after the onset of hepatitis are often insufficient to control HBV reactivation, preemptive antiviral therapy guided by regular HBV DNA monitoring, whereby the antiviral drug is given immediately when HBV DNA becomes detectable, is recommended by some guidelines to prevent hepatitis due to HBV reactivation [20, 21]. However, the definition of HBV reactivation and cut-off values of HBV DNA levels, along with the timing of initiation of antiviral treatment in patients with resolved HBV infection, have not been fully investigated yet.

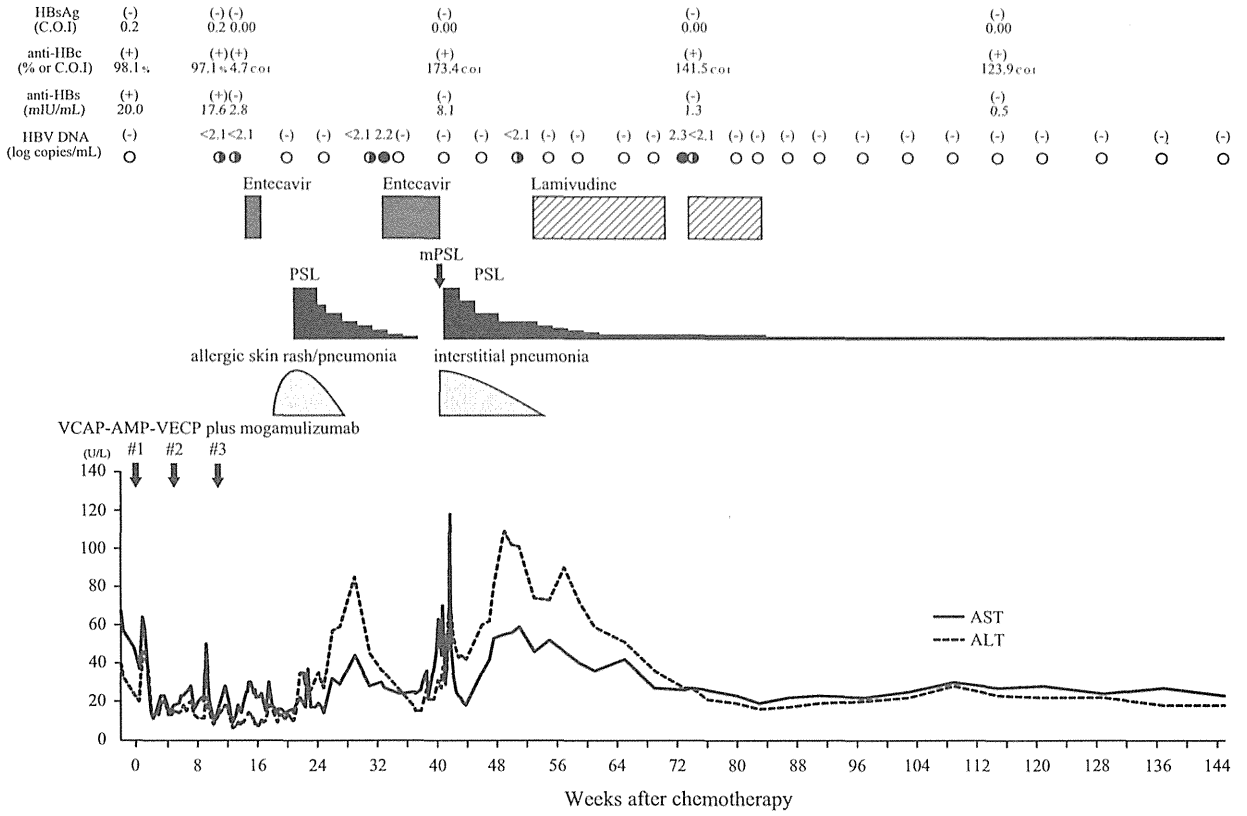

Fig. 2 Clinical course of case 1. A 65-year-old male was diagnosed as having adult T-cell leukemia–lymphoma of lymphoma type and received VCAP-AMP-VECP plus mogamulizumab combined chemotherapy. At 3 months after systemic chemotherapy, HBV reactivation was confirmed with HBV DNA levels below 2.1 log copies/mL and antiviral therapy (entecavir, 0.5 mg/day) was given immediately with no HBV-related hepatitis. He presented with elevation of transaminase levels after detection of HBV DNA, it considered not viral hepatitis but drug-induced liver damage because of transient and slight increase of HBV DNA levels. Because he suffered from an allergic rash and interstitial pneumonia (IP), entecavir could not be continued. Consequently, reemergence of HBV (HBV DNA levels of 2.2 log copies/mL) was observed at 3 months after the first detection of HBV reactivation. However, he discontinued entecavir because of the occurrence of IP, and HBV reactivation was again observed. Lamivudine was given for HBV reactivation, but was discontinued due to mild renal dysfunction, which resulted again in replication of HBV (HBV DNA levels of 2.3 log copies/mL) at 18 months after initiating mogamulizumab-containing chemotherapy. The *open circles* show undetectable PCR signals during HBV DNA monitoring; the *half-filled circles* show PCR signals indicating HBV DNA levels below 2.1 log copies/mL; and the *filled circles* show detectable PCR signals indicating HBV DNA levels of 2.1 log copies/mL or more. *HBV* hepatitis B virus, *PSL* prednisolone, *mPSL* methylprednisolone, *AST* aspartate transaminase, *ALT* alanine aminotransferase, *VCAP-AMP-VECP* VCAP (vincristine, cyclophosphamide, doxorubicin, prednisolone)-AMP (doxorubicin, ranimustine, prednisolone)-VECP (vindesine, etoposide, carboplatin, prednisolone)

In conclusion, the incidence of HBV reactivation was 12.5 % in ATL patients with resolved HBV infection following systemic chemotherapy. In mogamulizumab era, further well-designed prospective studies are warranted to estimate the incidence of HBV reactivation and to establish regular HBV DNA monitoring-guided preemptive antiviral therapy for these patients.

Acknowledgments We would like to thank staff as follows: Ms. Chiori Fukuyama and Dr. Shintaro Ogawa (Nagoya City University Graduate School of Medical Sciences, Nagoya) for keeping and measurement of specimens on this study. We also thank Dr. Shiro Akinaga (Kyowa Hakko Kirin Co., Ltd., Tokyo) for his enlightening advice on this article. This study was supported in part by the Ministry of Health, Labour and Welfare of Japan (grant-in-aid H24-kanen-004 to M.M.) and the Ministry of Education, Culture, Sports Science and Technology of Japan (grant-in-aid for Scientific Research (C) No. 24591428 to S.K.) and grant-in-aid for National Cancer Center Research and Development Fund (No. 26-A-4 to T.I.).

Conflict of interest Shigeru Kusumoto received Research funding and honoraria from Kyowa Hakko Kirin Co., Ltd., and honoraria from Bristol-Myers Squibb. Takashi Ishida received research funding from Kyowa Hakko Kirin Co., Ltd., Bayer Pharma AG, and Celgene K.K. Ryuzo Ueda received research funding from Kyowa Hakko Kirin Co., Ltd. Yasuhito Tanaka received research funding from Bristol-Myers Squibb, and honoraria from Bristol-Myers Squibb. Shinsuke Iida received research funding from Kyowa Hakko Kirin Co., Ltd.

References

1. Lok AS, Liang RH, Chiu EK, Wong KL, Chan TK, Todd D. Reactivation of hepatitis B virus replication in patients receiving cytotoxic therapy. Report of a prospective study. Gastroenterology. 1991;100(1):182–8.
2. Hui CK, Cheung WW, Zhang HY, Au WY, Yueng YH, Leung AY, et al. Kinetics and risk of de novo hepatitis B infection in HBsAg-negative patients undergoing cytotoxic chemotherapy. Gastroenterology. 2006;131(1):59–68.
3. Yeo W, Chan TC, Leung NW, Lam WY, Mo FK, Chu MT, et al. Hepatitis B virus reactivation in lymphoma patients with prior resolved hepatitis B undergoing anticancer therapy with or without rituximab. J Clin Oncol. 2009;27(4):605–11 (Epub 2008/12/17).
4. Kusumoto S, Tanaka Y, Mizokami M, Ueda R. Reactivation of hepatitis B virus following systemic chemotherapy for malignant lymphoma. Int J Hematol. 2009;90(1):13–23 (Epub 2009/06/23).
5. Kusumoto S, Tanaka Y, Ueda R, Mizokami M. Reactivation of hepatitis B virus following rituximab-plus-steroid combination chemotherapy. J Gastroenterol. 2011;46(1):9–16 (Epub 2010/10/07).
6. Mitka M. FDA: increased HBV reactivation risk with ofatumumab or rituximab. JAMA. 2013;310(16):1664.
7. Ishida T, Utsunomiya A, Iida S, Inagaki H, Takatsuka Y, Kusumoto S, et al. Clinical significance of CCR4 expression in adult T-cell leukemia/lymphoma: its close association with skin involvement and unfavorable outcome. Clin Cancer Res. 2003;9(10 Pt 1):3625–34.
8. Ishii T, Ishida T, Utsunomiya A, Inagaki A, Yano H, Komatsu H, et al. Defucosylated humanized anti-CCR4 monoclonal antibody KW-0761 as a novel immunotherapeutic agent for adult T-cell leukemia/lymphoma. Clin Cancer Res. 2010;16(5):1520–31.
9. Yamamoto K, Utsunomiya A, Tobinai K, Tsukasaki K, Uike N, Uozumi K, et al. Phase I study of KW-0761, a defucosylated humanized anti-CCR4 antibody, in relapsed patients with adult T-cell leukemia–lymphoma and peripheral T-cell lymphoma. J Clin Oncol. 2010;28(9):1591–8.
10. Ishida T, Ueda R. Antibody therapy for Adult T-cell leukemia–lymphoma. Int J Hematol. 2011;94(5):443–52.
11. Ishida T, Joh T, Uike N, Yamamoto K, Utsunomiya A, Yoshida S, et al. Defucosylated anti-CCR4 monoclonal antibody (KW-0761) for relapsed adult T-cell leukemia–lymphoma: a multicenter phase II study. J Clin Oncol. 2012;30(8):837–42.
12. Motohashi K, Suzuki T, Kishimoto K, Numata A, Nakajima Y, Tachibana T, et al. Successful treatment of a patient with adult T cell leukemia/lymphoma using anti-CC chemokine receptor 4 monoclonal antibody mogamulizumab followed by allogeneic hematopoietic stem cell transplantation. Int J Hematol. 2013;98(2):258–60.
13. Nakano N, Kusumoto S, Tanaka Y, Ishida T, Takeuchi S, Takatsuka Y, et al. Reactivation of hepatitis B virus in a patient with adult T-cell leukemia–lymphoma receiving the anti-CC chemokine receptor 4 antibody mogamulizumab. Hepatol Res. 2014;44(3):354–7.
14. Shin IT, Tanaka Y, Tateno Y, Mizokami M. Development and public release of a comprehensive hepatitis virus database. Hepatol Res. 2008;38(3):234–43.
15. Hsu C, Tsou HH, Lin SJ, Wang MC, Yao M, Hwang WL, et al. Chemotherapy-induced hepatitis B reactivation in lymphoma patients with resolved HBV infection: a prospective study. Hepatology. 2014;59(6):2092–100.
16. Kusumoto S, Tanaka Y, Suzuki R, Watanabe T, Nakata M, Takasaki H, et al. Prospective nationwide observational study of hepatitis B virus (HBV) DNA monitoring and preemptive antiviral therapy for HBV reactivation in patients with B-cell non-Hodgkin lymphoma following rituximab containing chemotherapy: results of interim analysis. Blood. 2012; 120(21):abstract 2641.
17. Tsukasaki K, Utsunomiya A, Fukuda H, Shibata T, Fukushima T, Takatsuka Y, et al. VCAP-AMP-VECP compared with biweekly CHOP for adult T-cell leukemia–lymphoma: Japan Clinical Oncology Group Study JCOG9801. J Clin Oncol. 2007;25(34):5458–64.
18. Jo T, Ishida T, Takemoto S, Suzushima H, Uozumi K, Yamamoto K, et al. Randomized phase II study of mogamulizumab (KW-0761) plus VCAP-AMP-VECP (mLSG15) versus mLSG15 alone for newly diagnosed aggressive adult T-cell leukemia–lymphoma (ATL). J Clin Oncol 2013; 31: (suppl; abstr 8506).
19. Ishida T, Ueda R. Immunopathogenesis of lymphoma: focus on CCR4. Cancer Sci. 2011;102(1):44–50.
20. Oketani M, Ido A, Uto H, Tsubouchi H. Prevention of hepatitis B virus reactivation in patients receiving immunosuppressive therapy or chemotherapy. Hepatol Res. 2012;42(7):627–36 Epub 2012/06/13.
21. EASL clinical practice guidelines. Management of chronic hepatitis B virus infection. J Hepatol. 2012;57(1):167–85 Epub 2012/03/23.

Construction of an Aptamer Modified Liposomal System Targeted to Tumor Endothelial Cells

Mst. Naznin Ara,[a] Takashi Matsuda,[b] Mamoru Hyodo,[a] Yu Sakurai,[a] Noritaka Ohga,[c] Kyoko Hida,[c] and Hideyoshi Harashima*[,a,b]

[a] *Laboratory of Innovative Nanomedicine, Faculty of Pharmaceutical Sciences, Hokkaido University;* [b] *Laboratory for Molecular Design of Pharmaceutics, Faculty of Pharmaceutical Sciences, Hokkaido University; Kita 12, Nishi 6, Kita-ku, Sapporo, Hokkaido 060–0812, Japan: and* [c] *Division of Vascular Biology, Graduate School of Dental Medicine, Hokkaido University; Kita 13, Nishi 7, Kita-ku, Sapporo, Hokkaido 060–0812, Japan.*
Received April 30, 2014; accepted August 24, 2014

We describe herein the development of a high affinity and specific DNA aptamer as a new ligand for use in liposomal nanoparticles to target cultured mouse tumor endothelial cells (mTECs). Active targeted nanotechnology based drug delivery systems are currently of great interest, due to their potential for reducing side effects and facilitating the delivery of cytotoxic drugs or genes in a site specific manner. In this study, we report on a promising aptamer candidate AraHH036 that shows selective binding towards mTECs. The aptamer does not bind to normal cells, normal endothelial cells or tumor cells. Therefore, we synthesized an aptamer–polyethylene glycol (PEG) lipid conjugate and prepared aptamer based liposomes (ALPs) by the standard lipid hydration method. First, we quantified the higher capacity of ALPs to internalize into mTECs by incubating ALPs containing 1 mol%, 5 mol% and 10 mol% aptamer of total lipids and compared the results to those for unmodified PEGylated liposomes (PLPs). A confocal laser scanning microscope (CLSM) uptake study indicated that the ALPs were taken up more efficiently than PLPs. The measured K_d value of the ALPs was 142 nM. An intracellular trafficking study confirmed that most of the rhodamine labeled ALPs were taken up and co-localized with the green lysotracker, thus confirming that they were located in lysosomes. Finally, using an aptamer based proteomics approach, the molecular target protein of the aptamer was identified as heat shock protein 70 (HSP70). The results suggest that these ALPs offer promise as a new carrier molecule for delivering anti-angiogenesis drugs to tumor vasculature.

Key words aptamer based liposome; targeted drug delivery; tumor endothelial cell; heat shock protein 70 (HSP70); cell-based systematic evolution of ligands by exponential enrichment

Inhibiting angiogenesis is a promising strategy for the treatment of cancer and other disorders related to metastasis.[1)] Metastases are the cause of 90% of all human cancer deaths. Chemotherapy of cancer metastases, which can be effective in some patients, is often associated with significant toxicity, poor bio-distribution, an unusual pharmacokinetic profile, resistance and non-specificity.[2,3)] Major progress in the treatment of cancer has been achieved over the past decades. In this context, the first angiogenesis inhibitors were reported in the 1980s from Folkman Laboratories. In 2004, the Food and Drug Administration (FDA) approved first aptamer drugs and Pegaptinib arrived on the market for the treatment of the wet (neovascular) form of age related macular degeneration (AMD). Many angiogenesis inhibitors are currently in the advanced clinical level research, and continuous efforts are needed to improve cancer therapy with regard to patient safety.[1,4)] Our goal in this study was to evaluate an aptamer ligand for trageting our recently isolated tumor endothelial cells, with the objective of developing a new active targeted drug delivery system.

Among the known drug delivery systems, liposomes are the most successful nanotechnology-based drug delivery system. Twelve liposomal drug products have already been launched in the world and many liposomal drugs are currently in the clinical trial stage.[5)] Liposome nanoparticles have been extensively studied as a tool or carrier for encapsulating drugs or genes. The addition of a conjugate of polyethylene glycol (PEG) linked to a lipid anchor (distearoylphosphatidylethanolamine) to the liposomal formulation was shown to significantly prolong liposome circulation time. PEG-coating contributes to stabilizing stress of the vesicles and provides important protection against opsonisation, resulting in delayed hepatic reticuloendothelial system (RES) clearance and greatly extending circulation time.[6)] Indeed, a hallmark of the long-circulating PEG-modified liposomal drug carriers are their enhanced accumulation in tumors.[7,8)] Ligand based liposomes are the most recent addition and technically well accepted vehicle for successful drug delivery.

Aptamers, which are short oligonucleotides either ssDNA or RNA, were first independently screened by a method involving the Systematic Evolution of Ligands by Exponential Enrichment (SELEX) by the two research groups Ellington, Szostak and Tuerk, Gold in 1990.[9,10)] The recently developed cell-based aptamer selection, termed cell-SELEX, uses intact living cancer cells as the target and closely related cells as controls to produce aptamers capable of identifying molecular differences between cancer cells.[11)] Over the last several years, aptamers have been recognized as an excellent, superior, fastest growing and promising new class of targeting ligand, especially in the nanotechnology platform for drug delivery in the area of cancer research. Since they possess several advantages as a targeting ligand, even over other ligands that are used in drug delivery, such as antibodies which were described by Cullen and Greene.[12)] The binding of an aptamer to a target is very selective and occurs with a high affinity. Aptamers can be chemically modified to enhance their stability in biological

The authors declare no conflict of interest.

* To whom correspondence should be addressed. e-mail: harasima@pharm.hokudai.ac.jp

fluids, to have a low or non immunogenicity, versatile synthetic accessibility, thermal stability, because of their small size, they can easily and rapidly diffuse into tissues and organs, thus permitting faster targeting in drug delivery.[13,14] To date, a variety of aptamers against different cancer cells have been isolated based on whole cell-SELEX, but only a very few of them have been tested for use in drug delivery.[15,16]

The objective of the present study was to target the tumor vasculature, which is an attractive and challenging target for the delivery of anticancer agents. When nanoparticles are injected intravenously to target cancer cells, they must penetrate cross the endothelial cells lining against oncotic pressure that is generated from inside the tumor microenvironment. At the same time, for *in vivo* applications, it is important for the therapeutic reagents to target only a particular cell type, thereby limiting side effects that result from nonspecific delivery. It would be possible to solve this problem by targeting the vasculalture.[17,18] Considering this, we examined a newly identified aptamer candidate AraHH036 that selectively binds to cultured tumor endothelial cells and implemented these aptamer conjugated liposomal nano particles as a carrier to target the tumor vasculature. We evaluated the uptake capacity, the binding affinity and the intracellular distribution of such a system to evaluate whether it could be used to deliver anticancer agents.

MATERIALS AND METHODS

Isolation of Mouse Tumor Endothelial Cells (mTECs) All experiments involving animals and their care were carried out consistent with Hokkaido University guidelines, and protocols approved by the Institutional Animal Care and Use Committee. Endothelial cells were isolated as previously described.[19–23] Briefly, normal skin endothelial cells (skin-ECs) were isolated from the dermis as controls. mTECs were isolated by magnetic bead cell sorting using an IMag cell separating system (BD Biosciences, San Jose, CA, U.S.A.). CD31-Positive cells were sorted and plated on 1.5% gelatin-coated culture plates and grown in EGM-2 MV (Clonetics, Walkers, MD, U.S.A.) and 15% fetal bovine serum (FBS). Diphtheria toxin (DT) (500 ng/mL, Calbiochem, San Diego, CA, U.S.A.) was added to the TEC subcultures to kill any remaining human tumor cells. Human cells express heparin-binding epidermal growth factor (EGF)-like growth factor (hHB-EGF), a DT-receptor. However, DT does not interact with mouse HB-EGF and murine ECs therefore survive this treatment.

Cells and Cell Lines We used primary cultured skin-ECs that were isolated from normal mice skin as a negative control. Primary cultured mTECs as target for selection, were isolated from human tumor xenografts of melanoma tumor cells (A375) into nude mice. A375, a super-metastatic human malignant melanoma cell, was a kind gift from Dr. Isaiah J. Fidler (University of Texas, M.D. Anderson Cancer Centre, Houston). OS-RC-2, human renal clear carcinoma cells were purchased from the RIKEN Cell Bank (Tsukuba, Japan). NIH3T3 cells were obtained from the American Type Culture Collection (Manassas, VA, U.S.A.).

Maintenance of Cell Cultures Primary cultured mTECs and normal skin-ECs were cultured using a special medium, namely EGM-2 MV (Lonza). Human renal cell carcinoma, OS-RC-2 cells were cultured in RPMI-1640, containing 10% fetal bovine serum. NIH3T3 and A375 cells were cultured in Dulbecco's modified Eagle's medium (DMEM) containing 10% fetal bovine serum. To prevent microbial growth, penicillin (100 unit/mL) and streptomycin (100 μg/mL) were added to all cell culture media. Cell cultures were maintained at 37°C in a 5% CO_2 incubator at 95% humidity. For regular cell cultures a 0.1% trypsin solution was used to dissociate the cells from the surface of the culture dish. However, RepCell was used (Cell Seed Inc., Tokyo, Japan) during the entire selection of a DNA aptamer, flow cytometry assay and during aptamer targeted protein purification.

Selection of Aptamers The cell-SELEX method was used to isolate aptamers specific for primary cultured mTECs. The method for selection has been described previously.[9] Briefly, 200 pmol of an 82mer random ssDNA library with fluorescein isothiocyanate (FITC) tagged at the 5′-end and a biotin tag at the 3′-end in 1× selection buffer (500 μL), was used to start the selection. The random library was first heated in a thermo-block at 80°C for 10 min, and then cooled slowly to form a secondary structure, which was then incubated with the target cells on ice for 45 min. Only the target cell bound library was collected for the next cycle selection. A total of 12 rounds of selection was performed with 2 rounds of negative selection at the 11th and 12th rounds. Finally, the aptamers that were bound to the surface of the cells were eluted by heating at 95°C for 5 min. The bound DNA was purified by phenol-chloroform extraction followed by ethanol precipitation. Regular polymerase chain reaction (PCR) was optimized and used to amplify the bound libraries after each cycle of selection. Asymmetric PCR was used to generate ssDNA for the next round selection. Eventually, cloning and sequencing was performed to identify the desire aptamer candidates.

Binding Assay by Fluorescence Activated Cell Sorting (FACS) A FACS experiment was performed to check the binding capacity of the AraHH036 (5′-ATGGGGGGCAGT GTACGGCGCGCCGGTGT-3′) aptamer against primary cultured tumor endothelial cells, normal endothelial cells, normal cells and tumor cells. To perform the experiment, 200 pmol of aptamer and 200 pmol of zero cycle libraries was heated 80°C for 10 min, and cooled slowly to permit secondary structures to be formed. A five molar excess of yeast tRNA and bovine serum albumin (BSA) used as a nonspecific binding agent. The RepCell dishes that were used permit cells to be detached without the need for using trypsin that can damage cell surface proteins. 1.0×10^6 cells were incubated with aptamer and the control zero-cycle ssDNA library on ice for 45 min, respectively. The cells were spun down (5000×***g***, 5 min 4°C) to remove the supernatant that contained unbound DNA. The cells were washed three times with 1× selection buffer. Finally, we performed a fluorescence analysis of the sample on a FACSCalibur flow cytometer (BD Biosciences) in which 10000 events were counted.

Synthesis of Aptamer–Maleimide–PEG_{2000}–1,2-Distearoyl-*sn*-glycero-3-phosphoethanolamine (DSPE) Conjugates The aptamer (100 nmol) was conjugated by reacting it with a 5 fold excess of maleimide–PEG_{2000}–DSPE by gentle overnight soaking in a Bio-shaker at room temperature. The aptamer was purchased from Sigma-Genosys. For the conjugation reaction, the disulphide (S–S) bonds of the aptamer were first cleaved by the treatment with an excess TCEP solution on ice for 30–40 min. After the conjugation reaction, the excess

maleimide–PEG_{2000}–DSPE was removed by dialysis (MWCO 4000) against 1% sodium dodecyl sulfate (SDS), 50 mM phosphate buffer at pH 7 with the solvent being changed three times at 4 h intervals. Further dialysis (MWCO 3500–5000) was performed in 50 mM ammonium hydrogen carbonate buffer at pH 8.0 by changing the solvent three times at every 4 h intervals. The purified aptamer–lipid conjugate was ion-exchanged with Zip-Tip C18 and examined by agarose-gel electrophoresis and matrix assisted laser desorption/ionization-time of flight (MALDI-TOF) MS spectroscopy.

Preparation of Liposomes Liposome (LP) formulations were prepared by the standard lipid hydration method. The molar ratio of egg phosphatidylcholine (EPC), cholesterol (Chol) and rhodamine-1,3-dioleoyl-*sn*-glycerophosphoethanolamine (DOPE) was 70:30:1. About 1, 5 and 10 mol% of PEG_{2000}–DSPE or Aptamer–PEG_{2000}–DSPE of the total lipid was added to the lipid solutions during the preparation of the PLPs or ALPs, respectively. All lipids were dissolved in chloroform–ethanol solutions, and, a lipid film was prepared by evaporating all of the solvents under a stream of nitrogen gas. The dried lipid film was hydrated by adding *N*-(2-hydroxyethyl)piperazine-*N*′-2-ethanesulfonic acid (HEPES) buffer (10 mM, pH=7.4) for 10 min at room temperature, followed to the sonication for approximately 30 s to a min in a bath type sonicator (AU-25 C, Aiwa, Tokyo, Japan). The average size and diameter of liposomes were measured by using a Zetasizer Nano ZS ZEN3600 (Malvern Instrument, Worcestershire, U.K.).

Quantitative Cellular Uptake of ALPs in mTECs by Spectrofluorometry To perform a standard quantitative cellular uptake analysis, 4.0×10^4 cells were seeded per cm^2 in 24-well plates (Corning Incorporated, Corning, NY, U.S.A.), followed by incubating the plates overnight at 37°C in an atmosphere of 5% CO_2, and 95% humidity. On the next experimental day, medium from cells cultured in 24 well-plates was removed by aspiration and the cells then washed once with warm 1× phosphate buffered saline (PBS). Next, rhodamine labeled liposomal solution at different concentration was added to the cells, followed by incubation for 1 h at 37°C in an atmosphere of 5% CO_2, and 95% humidity. After 1 h of incubation, the cells were washed twice with 1× warm PBS supplemented with 100 nM cholic acid and the cells were then incubated with 1× reporter lysis buffer at −80°C for 20 min to achieve lysis. The lysed cells were placed on ice to melt. Finally, the lysed solution was centrifuged at 12000 rpm for 5 min at 4°C to remove cell debris. The efficiency of cellular uptake in terms of the Fluorescence intensity of rhodamine in the supernatant solution was measured using a FP-750 Spectrofluorometer (JASCO, Tokyo, Japan) at the excitation and emission range (550–590 nm).

Measurement of K_d of ALPs To measure the binding affinity of aptamer based liposomes (ALPs), 4.0×10^4 cells were seeded per cm^2 in 24-well plates (Corning Incorporated) and incubated overnight at 37°C in an atmosphere of 5% CO_2 and 95% humidity. On the next experimental day, different concentrations of rhodamine labeled liposomes (0–1875 nM) incubated with cells for 1 h. After incubation, the cells were washed twice with 1× PBS supplemented with 100 nM cholic acid. Finally, the mean fluorescence intensity of the ALPs to the target cells was used to calculate specific binding. PEGylated liposomes at same concentrations were used as a control. The equilibrium dissociation constant K_d was measured by fitting the dependence of the fluorescence intensity of specific binding to the concentration of the ligands to the equation $Y=B_{max}X/(K_d+X)$ using the Sigma Plot 12 (Systat Software Inc., U.S.A.).

Qualitative Cellular Uptake and Intracellular Distribution of ALPs in mTECs Confocal laser scanning microscopy was used to visualize the uptake of the ALPs and their intracellular distribution. The mTECs were first seeded in a 35 mm glass bottom dish with 2 mL of medium and then incubated for 24 h. The cell density was 2.0×10^5 cells/glass bottom dish. On the next experimental day, the cells were incubated with 5 mol% of the total lipid of the ALPs and PLPs in Krebs buffer for 1 h at 37°C under an atmosphere of 5% CO_2 at 95% humidity. To confirm the intracellular distribution, the cells were stained with LysoTracker green (DND-26) 1 (μg/mL) for 30 min at 37°C. After 2–3 washings with 1× PBS supplemented with 100 nM cholic acid, the cells were viewed and imaged by confocal laser scanning microscopy.

RESULTS

Confirmation of the High Affinity Binding Capacity of the Aptamer Ligand To check whether the isolated aptamer candidate AraHH036 has the capacity to bind to mTECs, we carried out a FACS experiment and the findings showed that the aptamer treated mTECs exhibited a high shift compared to the control zero cycle library (Fig. 1). It was very important to check the selectivity of this aptamer as to whether it binds to other cells or not. To answer this question, we carried out a FACS experiment under the same condition for this aptamer as above, but against normal endothelial cells, *i.e.*, a normal NIH3T3 cell line, A375 metastatic tumor cell lines and OS-RC-2 human renal cancer cell lines. This aptamer had no capacity to bind against any of the above cells, except against A375, where a slight binding was detected (Fig. 2). This result confirmed the selective binding and high binding affinity of this promising candidate with respect to mTECs and also indicates that the molecular target to which this aptamer bound is expressed on the mTECs but not on the other cell lines tested.

Synthesis of a DNA Aptamer Conjugate with Maleimide–PEG_{2000}–DSPE The aptamer–PEG_{2000}–DSPE was successfully synthesized by conjugating a 5′-thiol-modified

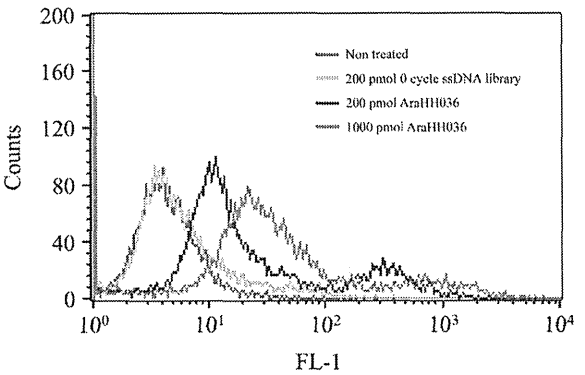

Fig. 1. Binding Assay of Aptamer AraHH036 against Target mTECs

A flow cytometry binding assay was performed, where the high affinity binding of FITC–aptamer at doses of 200 pmol and 100 pmol was observed. The zero cycle library at 200 pmol was used as a control.

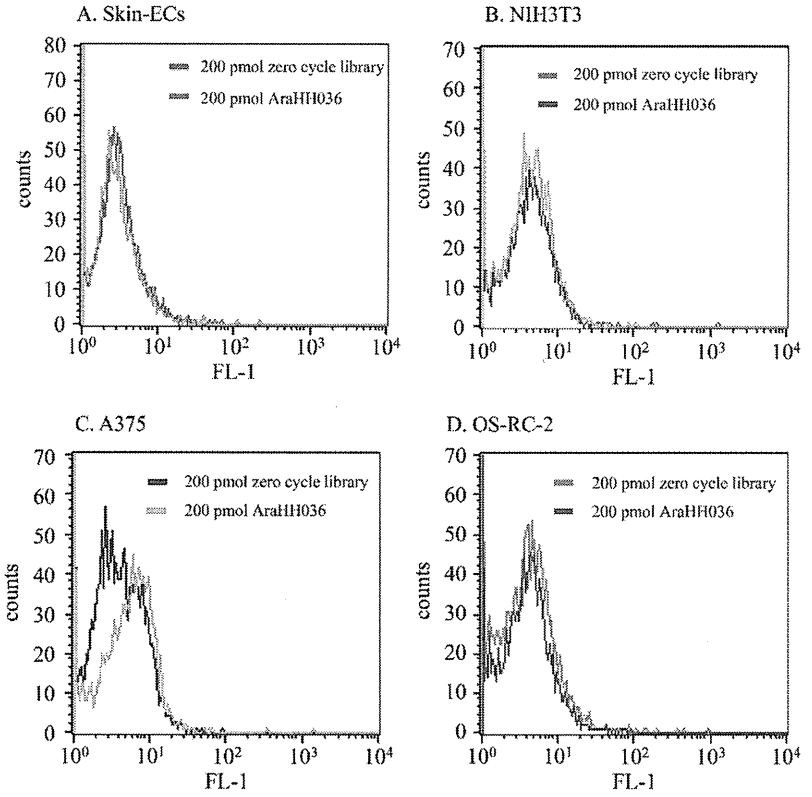

Fig. 2. Binding Assay of Aptamer AraHH036 to Normal Cells and Tumor Cells

Flow cytometry binding assay of aptamer at the dose 200 pmol. A. Normal skin-ECs, B. Normal NIH3T3, C. A375, D. OS-RC-2. In all cases, our aptamer show no binding. The 200 pmol zero cycle library was used as a control.

aptamer and 5 equimolar amounts of maleimide–PEG_{2000}–DSPE. We confirmed the conjugation as well as the molecular weight of the product by MALDI-TOF MS (Fig. 3). By applying dialysis using a 3500–5000 MWCO membrane, excess free lipid was successfully removed overnight. The final quantification of aptamer–PEG_{2000}–DSPE was done by UV-visible spectroscopy at 260 nm and the conjugated material was ready for preparing liposomes.

Preparation of Liposomes The standard lipid hydration method was successfully employed to prepare ALP. Zetasizer was used to analysis the particle size of ALP (Table 1). PEGylated liposomes without conjugating ligand was prepared as a control.

Quantitative Cellular Uptake Study of the ALP in mTECs Spectrofluorometry was used to perform the quantitative uptake assay. To evaluate the function of our constructed ALPs against primary cultured tumor endothelial cells, we first carried out an *in vitro* quantitative cellular uptake experiment using Rhodamine labeled 1, 5 and 10 mol% of the total lipid of ALP and PLP mTECs. The fluorescence intensity of the ALPs was found to be higher than that for PLP for three different doses compared to the control (Fig. 4). The enhanced cellular uptake in terms of fluorescence intensity was statistically significant compared to control PEG–LPs.

Measurement of the Binding Affinity (K_d) of the ALPs The mean fluorescence intensity for various concentrations of the rhodamine labeled ALP was measured. The experiments were repeated three times. The K_d value was 142 nM (Fig. 5). We also attempted to measure the K_d PLPs, but no binding with the mTECs was detected.

Qualitative Cellular Uptake and Intracellular Distribution of ALPs in mTECs To demonstrate the actual localization of the internalized ALP nano-carrier system, rhodamine labeled ALPs and PLPs were incubated for 1 h with mTECs. The mTECs were stained with green lysotracker. A confocal laser scanning microscope (CLSM) study showed that most of the internalized ALPs were merged with lysotracker, indicating that they were located in the lysosomal compartment; neither did PLPs show any affinity towards for mTECs nor were they merged or colocalized in the lysosomal compartment (Fig. 6).

DISCUSSION

To better understand the effects of the tumor microenvironment on the properties of endothelial cells and to understand how they are different from normal endothelial cells, our collaborative group isolated very pure tumor endothelial cells. Isolating and culturing tumor endothelial cells is a challenging task, because (i) endothelial cells are usually enmeshed in a complex type of tissue, consisting of vessel wall components, stromal cells, and tumor cells; and (ii) only a small fraction of cells within these tissues are actually endothelial cells. It is assumed that a single tumor endothelial cell can support many tumor cells.[19–23] Thus, to develop an anti-angiogenic therapy, for targeting endothelial cells might be a much more effective strategy than targeting the actual tumor cells themselves. In order to achieve vascular targeting, our strategy was to con-

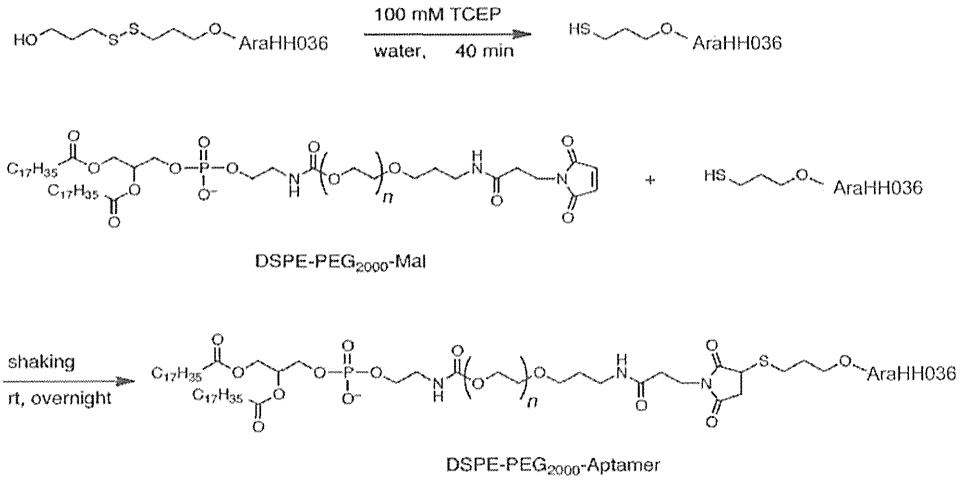

TCEP = tris(2-carboxyethyl)phosphine hydrochloride, efficient reducing agent for disulfide linkage

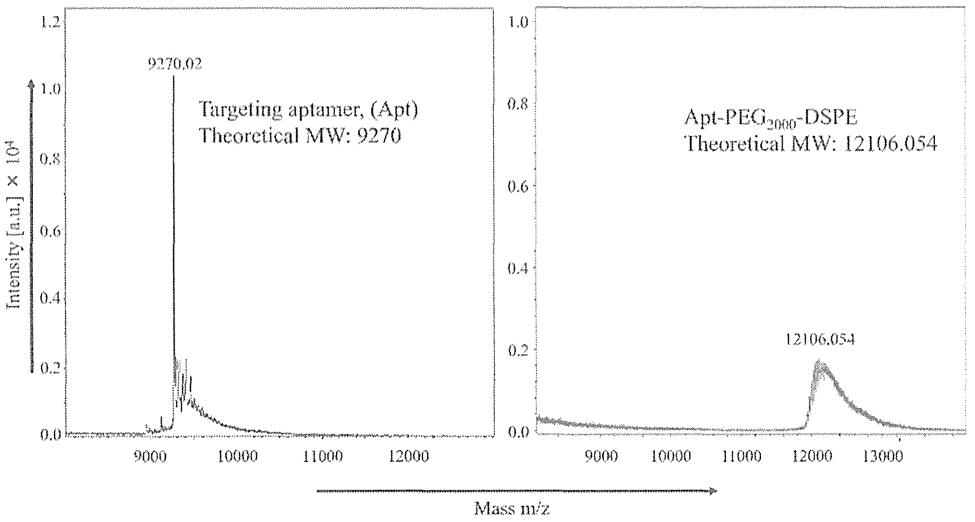

Fig. 3. Conjugation of the Aptamer–PEG_{2000}–DSPE

(A) Synthesis of the thiol modified aptamer AraHH036 with maleimide–PEG_{2000}–DSPE. Reduced aptamer and excess maleimide–PEG_{2000}–DSPE were reacted in water overnight at 37°C. (B) MALDI-TOF MS spectrometry was employed to confirm the conjugation.

Table 1. Physical Properties of Liposomes

Particle data		
Name of liposome	Size (nm)	ZP (mV)
PLPs	99±10	−19±6
ALPs	100±8	−28±7

struct an active targeting liposomal nano-carrier system.

It was recognized that a technique for increasing the selectivity of the interaction of the liposomes with diseased cells was desirable. Ligand based active targeting is the most powerful and a better option for achieving the selective and highest therapeutic efficacy with minimal adverse effets *via* receptor mediated endocytosis.[24] In this present study, we attempted to utilize our recently screened DNA aptamer ligand AraHH036 for the first time, to construct a new ligand based targeted PEGylated liposomal nano-carrier system and to carry out a functional analysis. In cell-based selection one common phenomena reflects many sequences for a single target with maximum similarity and, or, many sequences for many different targets due to an affinity and different binding moiety towards the target. In our case, the similarity within the different sequences was minimal, which may be due to the binding of aptamer candidates to the different targets expressed on the surface of the primary cultured tumor endothelial cells. At the same time, it should be noted that, in an earlier study, we found one very promising candidate AraHH001 for targeting to primary cultured tumor endothelial cells.[25] However, we also identified some other promising candidates with different sequences and minimal similarity, therefore, we continued our analysis and only recently concentrated on this promising aptamer ligand AraHH036 in an attempt to identify a new liposomal nanocarrier for vascular tergeting. We first investigated the binding capacity of the FITC-labeled aptamer for cultured tumor endothelial cells using a standard flow cy-

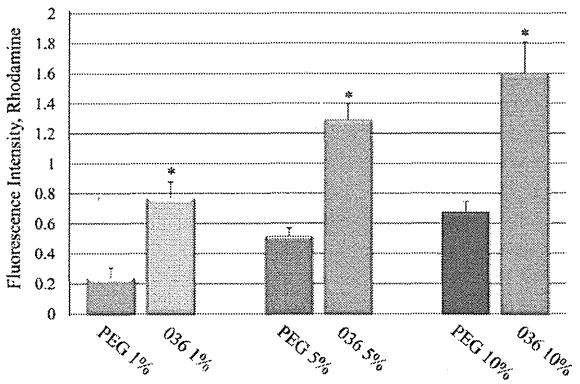

Fig. 4. Quantitative Cellular Uptake Assay for ALPs & PLPs

SM-ECs, 4.0×10^4/24-well were treated with 5 mol% of the total lipid of ALPs or PLPs for 1 h at 37°C. The cellular uptake is expressed as mean±S.D. The statistical analyses performed in a pair of cellular uptake of PEG- and aptamer-modified liposomes at each concentration by unpaired Student's *t*-test ($p<0.05$ *vs.* PEGylated liposome, $n=3$).

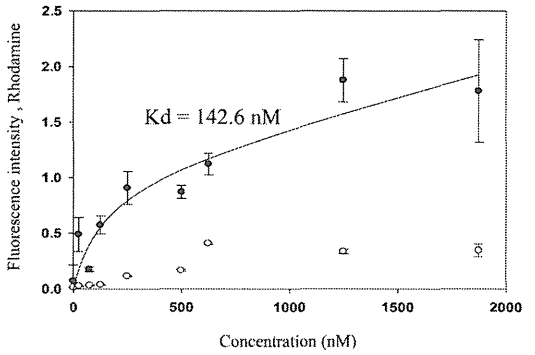

Fig. 5. Determination of Binding Affinity, the K_d Value of ALPs

mTECs were treated with various concentrations of ALPs or PLPs labeled with rhodamine DOPE. The average rhodamine intensity of the ALPs or PLPs *versus* varying concentrations were plotted to determine the dissociation constant, K_d. The experiment was repeated three times.

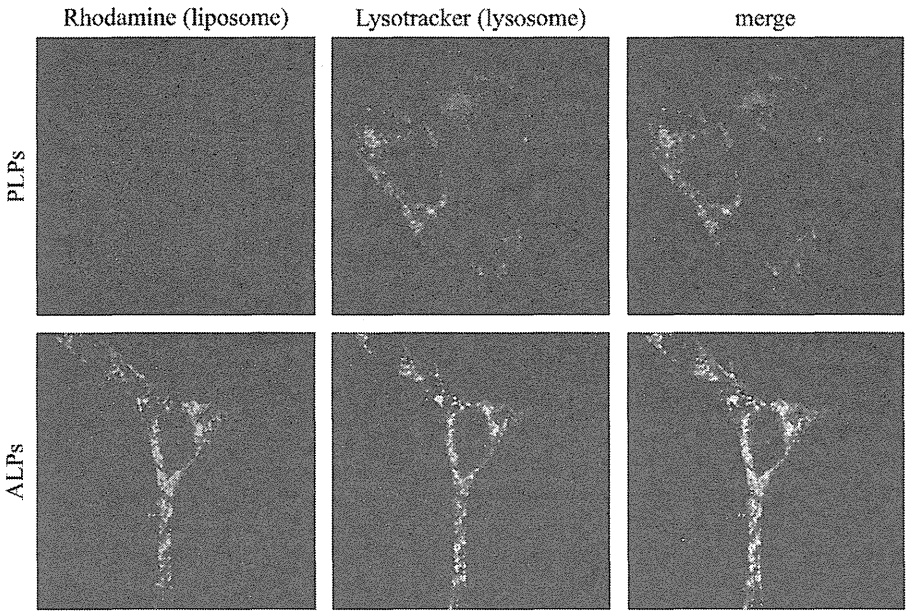

Fig. 6. A CLSM Uptake Assay and Intracellular Trafficking of ALPs

SM-ECs, 2.0×10^5 10/35 mm glass bottom was treated with 5 mol% of the total lipid of ALPs or PLPs for 1 h at 37°C. PEG–LPs and Apt–PEG–LPs containing rhodamine incubated with SM-ECs for 1 h at 37°C. Cells were stained with Green Lysotracker for 30 min.

tometry assay. We observed a very high binding affinity for the mTECs (Fig. 1). We tested the selectivity of this ligand using the same FACS experiment using four different normal and tumor cells. No binding to these cells was detected (Fig. 2).

Liposomes are the most advanced and effective drug carrier for therapeutics. Therefore, we next prepared an aptamer modified PEGylated nano-carrier system by conjugating the 5′-thiol aptamer ligand at the maleimide–PEG terminus on the liposomes. First, we cleaved the aptamer–S–S bond to produce an aptamer–SH bond by treatment with a reducing agent TCEP. A NAP-column was used to purify the aptamer–SH which was then conjugated with maleimide–PEG_{2000}–DSPE. A purified aptamer–lipid conjugation was obtained by dialysis (MWCO 3500–5000). The molecular weight and purity of the conjugates was confirmed by MALDI-TOF spectroscopy (Fig. 3). Finally, the aptamer–lipid concentration was determined by UV-visible spectroscopy.

PEG chains interfere with both the coupling of ligands to the lipid bilayer and the interaction of these ligands with the intended biological targets. To improve the selectivity and cellular uptake, attaching the aptamer ligands to the surface of the PEG chains is a potentially valuable approach. These ligands, when coupled to the PEG terminus, do not interfere with the binding of ligands to their respective recognition molecules.[26] Although EPR effects are based on the structural features of the neovasculature, long circulating liposomes can passively accumulate in tumor tisseue, but PEGylation inhibits cellular uptake. Therefore, active targeting is a very promising and effective route to solving this problem and, at the same time, to take advantage of the long retaining properties of PEG. Finally, liposomes were prepared by the lipid hydra-

tion method and their physicochemical properties were confirmed by a Zetasizer (Table 1). Interestingly, as an amount of PEGylation increased, the cellular uptake parallelly increased. We observed similar increase in cellular uptake by PEGylation with liver endothelial cells.[27] This may be because of a unknown property of endothelial cells.

We also carried out cellular uptake studies, quantitatively and qualitatively by utilizing the ALPs and the PLPs nano carrier in primary cultured tumor endothelial cells. A one h uptake study using different concentrations of total lipids, such as 1, 5 and 10 mol% in the ALPs and PLPs were carried out using the mTECs. The uptake of the ALPs nano-carrier system by mTECs was significant, compared to that for the unmodified PEGylated nano-carrier system. The uptake of the ALPs was dose dependent. This result also indicates that the targeted aptamer first recognized the cellular surface of the target molecule and was then internalized. Next, to visualize the extent of enhanced cellular uptake we carried out an *in-vitro* qualitative CLSM uptake study (Fig. 4). The rhodamine labeled 5 mol% of total lipids of the ALPs was found to have a much higher internalization capacity in mTECs compared to unmodified PLPs. Therefore, the above results suggest that modifying the PEGylated liposomes with the targeting ligand is critical for the association of and enhanced internalization of the nano-carrier system by mTECs. At the same time, due to the steric repulsion of the PEG polymer in unmodified PEGylated liposomes, the extent of association to the target mTECs was decreased, and, as a result, the uptake efficacy was lower. We also determined the binding affinity, K_d value of our ALPs. The K_d value was in the nano molar range, 142 nM (Fig. 5).

We next carried out an intracellular trafficking experiment in which the uptake of rhodamine labeled ALPs was evaluated using lyosotracker green as an intracellular marker. A CLSM study of intracellular trafficking showed that most of the ALPs were co-localized with lysotracker green, appearing as yellow (Fig. 6). However, some remaining ALPs that were not colocalized (red) remained intact inside the cytoplasm. PLPs were not taken up substantially and therefore, it was difficult to determine whether or not they were colocalized.

Finally, we attempted to identify the binding target of the aptamer ligand that was expressed selectively on the surface of the mTECs. An aptamer based proteomic approach was successfully used to isolate the molecular target. MALDI-TOF MS analysis confirmed that the molecular target of this aptamer ligand is heat shock protein HSP70 (Suppl. Fig. 1). HSP70 is heat shock proteins or heat stress proteins consist of chaperons of approximately 70 kDa in size. HSP70 is cytoxic to tumor cells but not in normal cells. It plays a very important role in cancer relevant pathways.[28] This protein has been shown to be released from cells as the result of acute stress as well as being secrereted after exposure to a number of stimuli. This protein inhibits apoptosis and also plays a role in resistance to cancer chemotherapy. The intracellular expression of HSP70 in different tumor cells are well established. Among researchers, still contradictory matter when tumor cell surface expression issue comes.[29-31] The exact reason of its expression on the surface of cultured mTECs is not currently known. More experimental studies need to be done and remains to be clarified in the future.

CONCLUSION

We developed a high affinity and selective DNA aptamer AraHH036 by means of the cell-SELEX method. Utilizing this aptamer we successfully prepared an aptamer based PEGylated liposomal delivery system that targets cultured tumor endothelial cells. The results of the study indicate that active targeting is a potentially useful tool for enhancing cellular uptake, compared to unmodified PEGylated liposomes. The binding affinity of this newly designed ALP was found to be in the nanomolar range. This study also reports on the nature of the molecular target of this aptamer ligand, which is referred to as HSP70. Therefore, we conclude that this system is potentially very promising and could be useful for the active targeting and delivery of drugs and or, gene therapy in the future. At the same time, it also represents a good example of using an aptamer ligand and the identification of biomarkers in terms of understanding such events at the molecular level.

Acknowledgments This study was supported by Grants from the Special Education and Research Expenses of the Ministry of Education, Culture, Sports, Science and Technology of Japan. This study was also supported by Grant-in-Aid for Young Scientists (B, 11018330) from the Ministry of Education, Culture, Sports, Science and Technology of Japan. The authors also thank Dr. Milton S. Feather for his advice in writing the English manuscript.

REFERENCES

1) Ferrara N, Kerbel RS. Angiogenesis as a therapeutic target. *Nature*, **438**, 967–974 (2005).
2) Mehlen P, Puisieux A. Metastasis: a question of life or death. *Nat. Rev. Cancer*, **6**, 449–458 (2006).
3) Weigelt B, Peterse JL, van't Veer LJ. Cancer metastasis: Markers and models. *Nat. Rev. Cancer*, **5**, 591–602 (2005).
4) Folkman J. Angiogenesis, an organizing principle for drug discovery? *Nat. Rev. Drug Discov.*, **6**, 273–286 (2007).
5) Chang HI, Yeh MK. Clinical development of liposome-based drugs: formulation, characterization, and therapeutic efficacy. *Int. J. Nanomedicine*, **7**, 49–60 (2012).
6) Woodle MC, Lasic DD. Sterically stabilized liposomes. *Biochim. Biophys. Acta*, **1113**, 171–199 (1992).
7) Gabizon A, Papahadjopoulos D. Liposome formulations with prolonged circulation time in blood and enhanced uptake by tumors. *Proc. Natl. Acad. Sci. U.S.A.*, **85**, 6949–6953 (1988).
8) Gabizon A, Martin F. Polyethylene glycol-coated (PEGylated) liposomal doxorubicin. *Drugs*, **54** (Suppl. 4), 15–21 (1997).
9) Ellington AD, Szostak JW. *In vitro* selection of RNA molecules that bind specific ligands. *Nature*, **346**, 818–822 (1990).
10) Tuerk C, Gold L. Systematic evolution of ligands by exponential enrichment, RNA ligands to bacteriophage T4 DNA polymerase. *Science*, **249**, 505–510 (1990).
11) Shangguan D, Li Y, Tang Z, Cao ZC, Chen HW, Mallikaratchy P, Sefah K, Yang CJ, Tan W. Aptamers evolved from live cells as effective molecular probes for cancer study. *Proc. Natl. Acad. Sci. U.S.A.*, **103**, 11838–11843 (2006).
12) Cullen BR, Greene WC. Regulatory pathways governing HIV-1 replication. *Cell*, **58**, 423–426 (1989).
13) Tan W, Wang H, Chen Y, Zhang X, Zhu H, Yang C, Yang R, Liu C. Molecular aptamers for drug delivery. *Trends Biotechnol.*, **29**, 634–640 (2011).
14) Zhang Y, Hong H, Cai W. Tumor targeted drug delivery with aptamers. *Curr. Med. Chem.*, **18**, 4185–4194 (2011).

15) Zhou J, Rossi JJ. Cell-specific aptamer targeted drug delivery. *Oligonucleotides*, **21**, 1–10 (2011).
16) Reinemann CS. Aptamer-modified nanoparticle and their use in cancer diagnostic and treatment. *Swiss Med. Wkly.*, **144**, 1–12 (2014).
17) Burdick MM, McCarty OJT, Jadhav S, Konstantopoulos K. Cell–cell interactions in inflammation and cancer metastasis. *IEEE Eng. Med. Biol. Mag.*, **20**, 86–91 (2001).
18) Siegel G, Malmsten M. The role of the endothelium in inflammation and tumor metastasis. *Int. J. Microcirc. Clin. Exp.*, **17**, 257–272 (1997).
19) Hida K, Klagsbrun M. A new perspective on tumor endothelial cells, unexpected chromosome and centrosome abnormalities. *Cancer Res.*, **65**, 2507–2510 (2005).
20) Hida K, Hida Y, Shindoh M. Understanding tumor endothelial cell abnormalities to develop ideal anti-angiogenic therapies. *Cancer Sci.*, **99**, 459–466 (2008).
21) Akino T, Hida K, Hida Y, Tsuchiya K, Freedman D, Muraki C, Ohga N, Matsuda K, Akiyama K, Harabayashi T, Shinohara N, Nonomura K, Klagsbrun M, Shindoh M. Cytogenic abnormalities of tumor-associated endothelial cells in human malignant tumors. *Am. J. Pathol.*, **175**, 2657–2667 (2009).
22) Matsuda K, Ohga N, Hida Y, Muraki C, Tsuchiya K, Kurosu T, Akino T, Shih S-C, Totsuka Y, Klagsbrun M, Shindoh M, Hida K. Isolated tumor endothelial cells maintain the specific character during long-term culture. *Biochem. Biophys. Res. Commun.*, **394**, 947–954 (2010).
23) Suzuki Y, Ohga N, Morishita Y, Hida K, Miyazono K, Watabe T. BMP-9 induces proliferation of multiple types of endothelial cells *in vitro* and *in vivo*. *J. Cell Sci.*, **123**, 1684–1692 (2010).
24) Allen TM, Cullis PR. Liposomal drug delivery systems: From concept to clinical applications. *Adv. Drug Deliv. Rev.*, **65**, 36–48 (2013).
25) Ara MN, Hyodo M, Ohga N, Hida K, Harashima H. Development of a novel DNA aptamer ligand targeting to primary cultured tumor endothelial cells by a cell-based SELEX method. *PLoS ONE*, **7**, e50174 (2012).
26) Nallamothu R, Wood GC, Pattillo CB, Scott RC, Kiani MF, Moore BM, Thoma L. A tumor vasculature targeted liposome delivery system for Combretastin A4: Design, characterization, and *in vitro* evaluation. *AAPS PharmSciTech*, **7**, E7–E16 (2006).
27) Akhter A, Hayashi Y, Sakurai Y, Ohga N, Hida K, Harashima H. A liposomal delivery system that targets liver endothelial cells based on a new peptide motif present in the ApoB-100 sequence. *Int. J. Pharm.*, **456**, 195–201 (2013).
28) Murphy ME. The HSP70 family and cancer. *Carcinogenesis*, **34**, 1181–1188 (2013).
29) Bayer C, Liebhardt ME, Schmid TE, Trajkovic-Arsic M, Hube K, Specht HM, Schilling D, Gehrmann M, Stangl S, Siveke JT, Wilkens JJ, Multhoff G. Validation of a heat shock protein 70 as a tumor specific biomarker for monitoring the outcome of radiation therapy in tumor mouse models. *Int. J. Radiat. Oncol. Biol. Phys.*, **88**, 694–700 (2014).
30) Multhoff G, Hightower LE. Distinguishing integral and receptor-bound heat shock protein 70 (Hsp 70) on the cell surface by Hsp70 specific antibody. *Cell Stress Chaperones*, **16**, 251–255 (2011).
31) Stangl S, Ghermann M, Riegger J, Kuhs K, Riederer I, Sievert W, Hube K, Mocikat R, Dressel R, Kremmer E, Pockley AG, Friedrich L, Vigh L, Skerra A, Multhoff G. Targeting membrane heat-shock protein 70 (Hsp 70) on tumors by cmHsp 70.1 antibody. *Proc. Natl. Acad. Sci. U.S.A.*, **108**, 733–738 (2011).

International Journal of Pharmaceutics 475 (2014) 227–237

Contents lists available at ScienceDirect

International Journal of Pharmaceutics

journal homepage: www.elsevier.com/locate/ijpharm

Pharmaceutical nanotechnology

Ligand density at the surface of a nanoparticle and different uptake mechanism: Two important factors for successful siRNA delivery to liver endothelial cells

Afsana Akhter [a], Yasuhiro Hayashi [a], Yu Sakurai [a], Noritaka Ohga [b], Kyoko Hida [b], Hideyoshi Harashima [a,b,*]

[a] Laboratory of Innovative Nanomedicine, Faculty of Pharmaceutical Sciences, Hokkaido University, Kita 12, Nishi 6, Kita-ku, Sapporo 060-0812, Japan
[b] Laboratory for Molecular Design of Pharmaceutics, Faculty of Pharmaceutical Sciences, Hokkaido University, Kita-12, Nishi-6, Kita-ku, Sapporo, Hokkaido 060-0812, Japan

ARTICLE INFO

Article history:
Received 29 April 2014
Received in revised form 8 August 2014
Accepted 23 August 2014
Available online 26 August 2014

Keywords:
ApoB 100
KLGR peptide
Liver sinusoidal endothelial cell
siRNA

ABSTRACT

The specific delivery of a gene to liver sinusoidal endothelial cells (LSEC) could become a useful strategy for treating various liver diseases associated with such cells. We previously reported that the accumulation of KLGR peptide modified liposomes through liver sinusoidal blood vessels was enhanced after an intravenous administration. Here, we report on an attempt to develop an LSEC targeted nanocarrier system to deliver siRNA for the successful knockdown of LSEC specific gene expression. The system involved the development of a multifunctional envelop-type nano device (MEND) modified with the KLGR peptide for siRNA delivery targeting LSEC. Our developed carrier successfully lowered specific gene expression in LSEC. An in vivo study showed that at a lower density of ligand at the surface of the MEND resulted in the highest knockdown of gene expression in LSEC. This is the first report of the successful delivery of siRNA to LSECs. Further experiments suggest that not only a higher endosomal escape efficiency into the cytosol but also the uptake mechanism as a function of ligand density are two important factors to be considered for targeting LSEC.

1. Introduction

Liver sinusoidal endothelial cells (LSECs) are located at the liver sinusoids where they separate hepatocytes from the blood flow. They play important role under normal physiological conditions as well as in many pathophysiological situations (DeLeve, 2011; March et al., 2009). Upon exposure to a variety of chemical toxins or a viral infection or when stimulated by cytokines or chemokines, they undergo into a huge change in gene expression and are thus active participants in inflammatory conditions (Ramadori et al., 2008; Neumann et al., 2011; Samantha et al., 2009; Neubauer et al., 2000). Disturbances in normal LSEC functions contribute to a wide range of pathophysiological alterations. For example, altered microcirculation due to changes in the porosity of LSEC has been implicated in alcoholic liver disease (Oshita et al., 1992). Despite the fact that they initiate different hepatic diseases, LSEC induce disease progression by playing active role in terms of immunity and inflammation (Neumann et al., 2011). To normalize the altered physiology or to reduce the induction of inflammation during various pathophysiological conditions, gene delivery to LSEC could become a useful therapeutic agent (Kren et al., 2009). This approach however has not been successful because a suitable specific carrier is not currently available. Though there are several reports of attempts of gene delivery to LSEC, only a few were successful in causing the knockdown of target gene expression. However, in this study we report on the development of a targeted nanocarrier that is specific to LSEC.

In the area of gene delivery, siRNA delivery has proved to be advantageous in terms of efficacy. One of the main obstacles for this therapy is specificity. Though no successful report of the in vivo delivery of siRNA to LSEC, some carrier mediated non-viral approaches have been successful in delivering plasmid DNA or oligonucleotide (ODN) to LSEC but failed to achieve the successful lowering of the expression of target gene (Takei et al., 2004). LSECs

* Corresponding author at: Faculty of Pharmaceutical Sciences, Hokkaido University, Kita-12, Nishi-6, Kita-ku, Sapporo, Hokkaido 060-0812, Japan. Tel.: +81 11 706 3919; fax: +81 11 706 4879.
E-mail address: harasima@pharm.hokudai.ac.jp (H. Harashima).

http://dx.doi.org/10.1016/j.ijpharm.2014.08.048
0378-5173/

possess unique receptors that recognize and internalize hyaluronic acid (HA). This HA modified targeted poly-L-lysine grafted-HA/DNA complex can be delivered to LSEC via receptor mediated endocytosis which results in the successful delivery of a gene inside the cell (Takei et al., 2004). In the present study, a multifunctional type nano device or MEND was used as the siRNA carrier. For this purpose we used a previously reported YSK05-MEND, which was reported to show successful RNAi activity in the liver (Sato et al., 2012). Our previous studies showed that YSK05 lipid facilitates the endosomal escape of the MEND and thus, enhances the efficacy of siRNA delivery into the cytosol and gene silencing (Sato et al., 2012; Sakurai et al., 2013)

To increase the specificity of the MEND, we modified the surface of the YSK05-MEND with a ligand that is selective for LSEC. For this purpose, previously reported LSEC targeting KLGR peptide was used (Akhter et al., 2013). This peptide ligand was designed from the ApoB-100 sequence of an LDL molecule, which is responsible for the binding of LDL molecules to LDL receptors (Urban et al., 1993, 2010). In the present study, stearylated KLGR (STR-KLGR) modified YSK05-MEND was able to deliver Tie2 siRNA into LSEC to suppress the endothelial cell specific Tie2 gene which is also known as the angiopoietin receptor protein (Peters et al., 2004). The delivery of Tie2 siRNA to the liver caused a significant decrease in the expression of the Tie2 gene which establishes selectivity of the STR-KLGR modified YSK05-MEND to LSEC. In this study, we made an additional effort, not only to verify the selectivity of the carrier for LSEC and not for hepatocytes but also optimized the carrier to achieve maximum gene silencing activity.

2. Materials and methods

2.1. Materials

F7 siRNA (sense strand): 5′-GGAUCAUCUCAAGUCUUACdTdT-3′ and Tie2 siRNA (sense strand): 5′-AUAUCUGGGCAAAUGAUGG-3′ was purchased from Sigma (Ishikari, Japan). RLTRKRGLKGGC (KLGR in brief) peptide and stearylated RLTRKRGLK (STR-KLGR) and stearylated octaarginine (STR-R8) peptides were purchased from Kurabo Industries, Osaka, Japan. 1,2-dimyristoyl-sn-glycerol, methoxyethyleneglycol 2000 ether (PEG-DMG), cholesterol (Chol) were purchased from Avanti Polar Lipids (Alabaster, AL, USA). *N*-[(3-Maleimide-1-oxopropyl)aminopropyl polyethyleneglycol-carbamyl] distearoylphosphatidyl-ethanolamine (maleimide-PEG-DSPE) was purchased from Nippon Oil and Fat Co. (Tokyo, Japan). Endothelial cell basal medium (EBM-2) and other related growth factors were purchased from Lonza (Walkersville, MD, USA). Dulbecco's fetal bovine serum (FBS) was obtained from Hyclone Laboratories (Logan, UT, USA). RiboGreen was purchased from Molecular Probes (Eugene, OR, USA). Trizol reagent was purchased from Invitrogen (Carlsbad, CA, USA). All other chemicals used in this study were of analytical grade.

2.2. Experimental animals

Male ICR mice were purchased from Japan SLC (Shizuoka, Japan). The experimental protocols were reviewed and approved by the Hokkaido University Animal Care Committee in accordance with the guidelines for the care and use of laboratory animals.

2.3. Cell culture

Hepa1–6 cells were obtained from the American Type Culture Collection (Manassas, VA) and the cells were maintained with Dulbecco's modified Eagle's medium (DMEM) supplemented with 10% fetal bovine serum and penicillin (100 units/ml) under an atmosphere of 5% CO_2 at 37 °C. Liver sinusoidal endothelial cells (LSEC) were maintained in EGM-2 (Lonza) supplemented with 5% FBS and other relevant growth factors. The cells were cultured under an atmosphere of 5% CO_2 at 37 °C (Hida et al., 2004; Akino et al., 2009; Ohga et al., 2009).

2.4. Conjugation of the KLGR peptide to PEG_{2000}-DSPE

Conjugation was achieved by incubating a 1.2:1 molar ratio of RLTRKRGLKGGC peptide and maleimide-PEG-DSPE in deionized water at room temperature for 24 h. The conjugation of KLGR peptide with PEG was confirmed by matrix assisted laser desorption/ionization–time of flight (MALDI–TOF) MS (Bruker Daltonics, Germany) using acetonitrile:water = 7:3 with 0.1% of trifluoroacetate as the matrix solution, supplied with a 10 mg/ml solution of dihydroxybenzoic acid.

2.5. MEND preparation

In this study, we used a YSK05-MEND that was previously reported by our laboratory (Sato et al., 2012). The YSK05 lipid, used to prepare liposomes contains one tertiary amine group and has pH-sensitive properties, and long, unsaturated carbon chains for emphasizing a cone shaped structure (Sato et al., 2012). MENDs were typically prepared using YSK05, a cationic lipid, cholesterol and PEG-DMG using a t-BuOH dilution procedure. The molar ratio of YSK05/cholesterol/PEG-DMG in the MEND was 70/30/3. To stabilize the lipid membrane during the formulation process and for preservation we used PEG-DMG. For the preparation of lipid layer 10 mM lipids were dissolved in a 90% t-BuOH solution. To prepare liposome cy3 labeled or unlabeled, the lipid solution was titrated slowly with an siRNA solution in 1 mM citrate buffer (pH 4.5) under vigorous mixing to permit the siRNA to be incorporated inside the lipid layer and the resulting suspension was then diluted quickly with citrate buffer to final concentration of <20% t-BuOH. The t-BuOH was removed by ultrafiltration, and the external buffer was replaced with phosphate buffered saline (PBS, pH 7.4). An empty MEND with the same lipid composition was prepared by a similar procedure, with the exception that the lipid solution was titrated with an equivalent volume of 1 mM citrate buffer instead of siRNA. For modifying the surface of the MEND with KLGR-PEG or STR-KLGR, the MENDs were incubated at 45 °C for 45 min with KLGR-PEG-DSPE or STR-KLGR. Labeled MENDs were prepared by adding 1 mol% of NBD-DOPE or rhodamine-DOPE to the lipid–t-BuOH solution prior to mixing with the siRNA. The average size and zeta potential of the MENDs were measured by a Zetasizer Nano ZS ZEN3600 (Malvern Instruments, Worcestershire, UK).

2.6. RiboGreen assay

For the determination of siRNA encapsulation efficiency of the developed MEND and to measure the concentration of siRNA, a RiboGreen fluorescence assay was performed (Toriyabe et al., 2013). RiboGreen (Molecular Probes, OR, U.S.A.) that binds specifically to double-stranded siRNA and produces a fluorescence intensity only when bound to siRNA. Fluorescence intensity was measured with a spectrofluorometer (Enspire 2300 multilabel Reader, Perkinelmer). First, MENDs were diluted to different concentration in 10 mM HEPES buffer at pH 7.4. Then RiboGreen was added to all the samples at a 1:1 ratio (v/v) either in the presence or absence of 0.1% (w/v) Triton X-100. A standard curve was prepared using different concentration of siRNA and the siRNA concentrations in all the samples were calculated from siRNA standard curve. siRNA encapsulation efficiency was measured by comparing the concentration of siRNA in the presence and absence of Triton X-100.